

Implicated Role of Endocytosis in the Internalization and
Intracellular Transport of Plasmid DNA During Electric Field-
Mediated Gene Delivery

by

Mina Wu

Department of Biomedical Engineering
Duke University

Date: _____

Approved:

Fan Yuan, Supervisor

Roger C. Barr

Christopher Dwyer

Kam Leong

William Reichert

Dissertation submitted in partial fulfillment of
the requirements for the degree of Doctor of Philosophy in the Department of
Biomedical Engineering in the Graduate School
of Duke University

2011

ABSTRACT

Implicated Role of Endocytosis in the Internalization and
Intracellular Transport of Plasmid DNA During Electric Field-
Mediated Gene Delivery

by

Mina Wu

Department of Biomedical Engineering
Duke University

Date: _____

Approved:

Fan Yuan, Supervisor

Roger C. Barr

Christopher Dwyer

Kam Leong

William Reichert

An abstract of a dissertation submitted in partial
fulfillment of the requirements for the degree
of Doctor of Philosophy in the Department of
Biomedical Engineering in the Graduate School
of Duke University

2011

Copyright by
Mina Wu
2011

ABSTRACT

Electric field mediated gene delivery (EFMGD) or electrotransfection is a popular, non-viral gene delivery method that has been used in a variety of studies and applications ranging from basic cell biology research to clinical gene therapy. Yet, the mechanism(s) by which electrotransfection facilitates DNA delivery across the cell membrane into the cell and its subsequent intracellular transport across the cytosolic space towards the nucleus have been insufficiently studied and still remain controversial. Understanding these mechanisms and characterizing the intracellular journey of pDNA is important for understanding the physiological barriers of EFMGD within the cell, which can be used to engineer better solutions to overcome these barriers with the ultimate goal of improving the transfection efficiency of this technology.

Conventional thought in the field assumes that such transport modes as diffusion, electrophoresis, and electro-osmosis, which govern the entry of small molecules into cells through electric field-generated transient membrane pores, also apply to electric field-mediated delivery of therapeutic DNA. We propose that electrically-induced gene transfer into cells is governed by an alternative, more active mode of transport that entails the involvement of cellular endocytic processes. It is our hypothesis that pulsed electric field generate these membrane pores which interact with

nearby DNA molecules; but that actual DNA translocation across the membrane is driven by endocytosis, which consequently, then, also plays a role in the intracellular transport of the DNA. To this end, we first investigated the dependence of electrotransfection efficiency (eTE) on binding of plasmid DNA (pDNA) to plasma membrane. Binding concentrates DNA molecules in the vicinity of the cell membrane, which should theoretically result in a greater number of DNA-membrane interactions during pulsed electric field, more internalized DNA, and ultimately, higher eTE values. We demonstrated that supplementing the electrotransfection buffer with divalent cations (Ca^{2+} and Mg^{2+}) is an effective method of promoting pDNA adsorption to the cell membrane. This cation-mediated increase in DNA adsorption to the cellular membrane resulted in a consequent increase in eTE, up to a certain threshold concentration for each cation. To determine the timeframe for completion of pDNA internalization following pulse treatment, trypsin treatment was applied to cells at different timepoints after electrotransfection to strip off any residual, membrane-bound pDNA that had not been internalized. Trypsin treatment at 10 min post electrotransfection still resulted in a significant reduction in eTE, indicating that the time period for complete cellular uptake far exceeded the lifetime (~ 10 msec) of electric field-induced transient pores. The role of endocytosis was further probed by noting the effect on eTE when cells were treated with three endocytic inhibitors (chlorpromazine, genistein, dynasore) targeting different internalization mechanisms or silenced of dynamin expression using specific, small

interfering RNA (siRNA). siRNA silencing and all three pharmacological inhibitors yielded substantial and statistically significant reductions in the eTE. Taken together, these findings suggest that the mechanism of electric-field mediated DNA internalization entails: (i) binding of pDNA to cell membrane and (ii) endocytosis of membrane-bound pDNA.

The same strategies of pharmacological endocytic inhibition and siRNA silencing was used to further explore and compare electric field-induced pDNA internalization in additional cell lines that differ in terms of cell type, proliferation rates, proliferative capacity (i.e. primary versus immortalized/cancer line), etc. in order to determine whether endocytosis is a universally implicated mechanism across many cell lines. Results showed different endocytic pathways to be recruited for pDNA uptake in a cell-dependent manner and that one or multiple pathways may contribute to uptake within a cell line.

Taken together, the studies presented in this dissertation provide both indirect and direct evidence suggesting an endocytic role in the translocation of pDNA across the cell membrane and its intracellular routing towards the nucleus for EFMGD. These seminal findings could potentially lead to better understanding of the intracellular barriers encountered by EFMGD, more strategic optimization of electrotransfection parameters than the trial-and-error approach currently used, and enhanced transfection efficiencies.

To Mom and Dad:

Thank you for your unconditional love and support

Table of Contents

| | |
|---|------------|
| Abstract | iv |
| List of Figures..... | xii |
| 1. Introduction..... | 1 |
| 2. Background..... | 5 |
| 2.1 Gene Delivery Approaches | 5 |
| 2.2 Fundamentals of Electroporation..... | 10 |
| 2.2.1 Electropermeabilization..... | 11 |
| 2.2.2 Transmembrane Transport of DNA | 12 |
| 2.3 Diffusion-negligible Intracellular Transport | 17 |
| 2.4 Endocytic Pathways | 20 |
| 2.4.1 Clathrin-mediated endocytosis | 21 |
| 2.4.2 Caveolae-mediated endocytosis..... | 23 |
| 2.4.3 Macropinocytosis | 25 |
| 2.4.4 Clathrin- and caveolae- independent endocytosis | 27 |
| 3. Membrane Binding of Plasmid DNA and Endocytic Pathways Are Involved in Electrotransfection of Mammalian Cells | 29 |
| 3.1 Introduction..... | 29 |
| 3.2 Materials & Methods..... | 32 |
| 3.2.1 Cell Culture | 32 |
| 3.2.2 Plasmid | 33 |
| 3.2.3 Membrane Adsorption of plasmid DNA | 34 |

| | |
|--|-----------|
| 3.2.4 Trypsin-Mediated Removal of Membrane-adsorbed DNA | 34 |
| 3.2.5 Electrotransfection..... | 35 |
| 3.2.6 Treatment of Cells with Pharmacological Inhibitors of Endocytosis..... | 36 |
| 3.2.7 Flow Cytometry | 37 |
| 3.2.8 Knockdown of Dynamin II Expression | 38 |
| 3.2.9 Western Blot Analysis..... | 38 |
| 3.2.10 Confocal Fluorescence Microscopy..... | 39 |
| 3.2.11 Statistical Analysis..... | 40 |
| 3.3 Results | 40 |
| 3.3.1 Effects of divalent cations on pDNA adsorption to cell membrane and electrotransfection. | 40 |
| 3.3.2 Slow internalization of pDNA after exposure to electric field..... | 44 |
| 3.3.3 Effects of endocytic inhibitors on electrotransfection efficiency. | 46 |
| 3.3.4 Dependence of electrotransfection efficiency on dynamin expression..... | 48 |
| 3.4 Discussion..... | 49 |
| 3.4.1 Effects of cations on pDNA delivery | 50 |
| 3.4.2 Effects of adsorbed pDNA on membrane surfaces | 54 |
| 3.4.3 Dynamics of pDNA internalization after exposure to electric field..... | 55 |
| 3.4.4 Effects of endocytic impairment on electrotransfection efficiency..... | 56 |
| 3.5 Conclusions | 58 |
| 4. Endocytic Pathways are Recruited for Electric Field-mediated DNA Uptake in a Cell-dependent Manner | 60 |
| 4.1 Introduction..... | 60 |

| | |
|---|-----------|
| 4.2 Materials & Methods..... | 62 |
| 4.2.1 Cell Culture | 62 |
| 4.2.2 Plasmid | 63 |
| 4.2.3 Electrotransfection..... | 64 |
| 4.2.4 Treatment of Cells with Pharmacological Inhibitors of Endocytosis..... | 64 |
| 4.2.5 Flow Cytometry | 66 |
| 4.2.6 Small, interfering RNA (siRNA) Transfection..... | 66 |
| 4.2.7 Western Blot Analysis..... | 69 |
| 4.2.8 Statistical Analysis..... | 70 |
| 4.3 Results | 70 |
| 4.3.1 Effect of endocytic inhibitors on electrotransfection efficiency. | 70 |
| 4.3.2 Effect of siRNA knockdown on electrotransfection efficiency | 73 |
| 4.4 Discussion..... | 78 |
| 4.4.1 Pharmacological inhibition of electrotransfected pDNA delivery | 78 |
| 4.4.2 Effect of siRNA silencing of endocytic proteins on electrotransfection efficiency | 83 |
| 4.5 Conclusions | 88 |
| 5. Future Works..... | 90 |
| 5.1 Visualization of the Effect of Endocytic Inhibition on Electric Field-mediated pDNA Uptake and Intracellular Distribution | 90 |
| 5.2 Visualization of Colocalization of Fluorescently-labeled Endocytic Vesicles and fluorescently-tagged plasmid DNA Following EFMGD | 92 |

| | |
|---|------------|
| 5.3 Pulsed Electric Field Parameter-dependent Recruitment of Endocytic Pathway(s) | 93 |
| References | 97 |
| Biography | 113 |

List of Figures

Figure 2.1: Pathways of endocytosis 28

Figure 3.1: Dependence of membrane-bound pDNA on cation concentrations. pDNA was labeled with YOYO 1 dye with basepair-to-DNA ratio of 5:1. The binding was characterized in terms of (A) percent of pDNA-associated cells and (B) average fluorescence intensity with arbitrary unit (a.u.) per pDNA-associated cell. The number of independent trials (n) was 5-6. The symbols and error bars denote mean and standard deviation, respectively. 41

Figure 3.2: Dependence of electrotransfection efficiency on cation concentrations. eTE is defined as the percent of live cells expressing GFP. B16-F10 cells were electrotransfected (400 V/cm, 5 msec, 8 pulses, 1 Hz) with GFP-encoding unlabeled pDNA in a transfection buffer. (A) The low ionic strength medium supplemented with Ca^{2+} or Mg^{2+} at varying concentrations was used as the electrotransfection buffer. N = 7-8. The symbols and error bars denote mean and standard deviation, respectively. The peak eTE value in each curve was significantly higher than those at both ends of the same curve ($P < 0.05$). In Panels (B) and (C), OptiMEM was used as the electrotransfection buffer. After 20 min incubation post electrotransfection, the cells were re-suspended in the low ionic strength medium supplemented with either Ca^{2+} or Mg^{2+} at varying concentrations, and treated again with the same electric field. The GFP expression was quantified at 24 hrs. n = 4. The filled circles denote data from individual samples, the "x" symbol represents the mean of the samples at a given cation concentration, and the line represents the linear regression of the mean data. The mean value was statistically independent of the variation in Ca^{2+} and Mg^{2+} concentrations ($P > 0.05$, Mann Whitney U test).. 43

Figure 3.3: Effects of trypsin treatment on pDNA adsorption to cell membrane and eTE. (A) YOYO 1-labeled pDNA (green) formed complexes with FM4-64FX labeled plasma membrane (red) following exposure of cells to pulsed electric field (400 V/cm, 5 msec, 8 pulses, 1 Hz). The image was taken shortly after the application of electric field. (B) The experimental protocol was the same as that in the Panel (A), except that at 10 min post electric field exposure, the cells were treated with 0.25% trypsin-EDTA solution for 30 min at 37°C. The image was taken after the trypsin treatment. (C) B16-F10 cells in pDNA solution were exposed to the same electric pulses (EP) as above. At 10 or 40 min post EP

exposure, the cells were treated with 0.25% trypsin for 30 min at 37°C. Then, the cells were cultured for 24 hrs at 37°C. The eTE was measured as the percent of live cells expressing GFP and normalized by the data from the no treatment group. The solid column and error bar represent mean and standard deviation of the relative eTE, respectively. n = 6 - 9. * P < 0.05 (Mann-Whitney U test).. 45

Figure 3.4: Reduction in cellular uptake of pDNA and the eTE by endocytic inhibitor treatment. pDNA covalently labeled with rhodamine (red) was electrotransfected (400 V/cm, 5 msec, 8 pulses, 1 Hz) into cells pre-treated with (A) DMSO (drug vehicle) or (B) dynasore (80 µM) for 1 hr. After electrotransfection, the cells were incubated at 37°C to enable cellular uptake of pDNA for 30 min. At the end of incubation, the cells were examined using confocal microscopy. Arrows in the microscopic images denote pDNA internalized by cells. To visualize three-dimensional distribution of pDNA in the cytosol, two optical cross-sections of DMSO-treated cells in x-z and y-z planes are shown in Panel (C). Effects of endocytic inhibitor treatment on the eTE are shown in Panel (D). Cells were treated with DMSO (Ctrl), 28 µM CPZ, 200 µM genistein (GE), or 80 µM dynasore (DN) for 1 hr prior to electrotransfection with the GFP-encoding pDNA. The eTE, defined as the percent of live cells expressing GFP, was quantified after cells were cultured at 37°C for 24 hrs. n = 4-6. * P<0.05 and **P<0.005(Mann-Whitney U test)..... 47

Figure 3.5: Effects of dynamin II knockdown on pDNA electrotransfection. B16-F10 cells were transfected with either the control siRNA or one of the two specific siRNA oligos directed against two different sequences (i.e., Sq1 and Sq2) in mouse dynamin II gene for silencing its expression. The siRNA treatment was followed by pDNA electrotransfection with a 48-hr delay. Dynamin II and β-actin (loading control) expression levels in Western blot analysis are shown in Panel A and normalized electrotransfection efficiencies are shown in Panel B. The bars and error bars indicate the means and standard deviations of 4 independent trials, respectively. The data from each trial, used in mean and standard deviation calculation, was the average value of replicates or triplicates. *, P < 0.05 (Mann-Whitney U test)..... 49

Figure 4.1: Effect of endocytic inhibitor treatment on electrotransfection efficiency (eTE). (A) HT29 cells were treated with 50 µM chlorpromazine (CPZ), 300 µM genistein, and

300 μ M amiloride, and (B) NHDFs were treated with 28 μ M CPZ, 200 μ M genistein, and 2.5 mM amiloride, or their equivalent volumes in drug vehicle DMSO (Control) for 1 hr prior to electrotransfection with GFP-encoding pDNA. Flow cytometry was used to quantify eTE after cells were cultured at 37°C for 24 hrs post-transfection. eTE, defined as the percent of live cells expressing GFP, for each drug treated group was normalized by their respective control. N = 4–7 independent trials. * P < 0.05 (Mann-Whitney U test)..... 72

Figure 4.2: Western blot of target protein knockdown. For each target protein, NHDF and HT29 cells were transfected with two specific siRNA oligos directed against two different sequences (i.e., siRNA-1 and siRNA-2) and control siRNA duplexes of comparable GC content. HT29 exhibited no band for Rab34 (most likely due to low endogenous expression levels) although non-specific bands were detected above and below the band of interest. Actin was used as the loading control. Representative images shown of two independent experiments..... 74

Figure 4.3: Effect of siRNA knockdown of caveolin-1 (CAV1), Rab34, and clathrin heavy chain (CHC) on electrotransfection efficiency of HT29. For each targeted protein, HT29 cells were transfected with either of two siRNA oligos (siRNA-1 and siRNA-2) directed against two different nucleotide sequences or the corresponding control siRNA. After siRNA transfection, cells were incubated for 48 hours and subjected to pDNA electrotransfection. siRNA oligos were grouped with the control siRNA of similar GC content in the chart above. Error bars denote standard error of N=4-5 independent trials. * denotes a statistically significant difference between the treated group and its control. P < 0.05 (Mann-Whitney U test)..... 77

Figure 4.4: Effect of siRNA knockdown of caveolin-1 (CAV1), Rab34, and clathrin heavy chain (CHC) on electrotransfection efficiency on NHDF. For each targeted protein, NHDF cells were transfected with either of two siRNA oligos (siRNA-1 and siRNA-2) directed against two different nucleotide sequences or the corresponding control siRNA. (A) For knockdown of CAV1 and Rab34, cells were transfected with 300 nM siRNA or control duplex using the Amaxa Nucleofector II and incubate 48 h before pDNA electrotransfection (B) For knockdown of CHC, cells were transfected with 1.2 μ M

siRNA or control duplex using the Amaxa Nucleofector on day 1, transfected again with 50 nM siRNA using Lipofectamine RNAiMax on day 3, and subjected to pDNA electrotransfection on day 5. siRNA oligos were grouped with the control siRNA of similar GC content in the charts above. Error bars denote standard error of 6-9 independent trials. * denotes a statistically significant difference between the treated group and its control. $P < 0.05$ (Mann-Whitney U test). LoGC(Ctrl1) and LoGC(Ctrl2) denotes control groups transfected with the Stealth control duplex of Low GC content, using the transfection protocols described in (A) and (B), respectively.78

Figure 5.1: Effect of chlorpromazine (50 μM , 1h) and genistein (300 μM , 1h) treatment on electrotransfection efficiency of HT29 for different electric field pulse regimens. N=2-3 trials for all groups except for '240V,5ms,6P' group (N=5-6 trials)..... 95

Chapter 1

INTRODUCTION

Non-viral gene therapy, which utilizes a genetic-based therapeutic approach to treating a variety of diseases, offers tremendous advantages over their viral counterparts in terms of cost-effectiveness, ease of production, stability, and safety, but its full potential is still stifled by poor transfection efficiency and gene expression. The efficacy and efficiency of non-viral gene therapy is highly determined by delivery of the therapeutic gene to its target cells and ultimately the nucleus for gene expression. Its transport, however, is hindered by a variety of physiological barriers along the way that all have the potential to reduce transfection efficiency. Electric field mediated gene delivery (EFMGD) or electrotransfection usually entails local administration of the therapeutic DNA near the target site followed by application of electric field pulses to induce DNA delivery into and transfection of target cells. In this case, pDNA must overcome, in sequential order: 1) the interstitial space, which is composed of the extracellular matrix (ECM) and cells that bind pDNA and physically inhibit diffusive and convective mobility of DNA, 2) the cell membrane of the target cells, which poses as a physical barrier to prevent entry of most exogenous molecules including foreign DNA, 3) the intracellular cytosol, which inhibit diffusive mobility of DNA due to cytoplasmic

crowding (organelles, proteins, cytoskeletal networks, etc.) and binding effects and cause pDNA degradation due to the presence of cytosolic nucleases, and 4) the nuclear envelope, which pose as another physical barrier to regulate entry of molecules into the nucleus (Henshaw and Yuan 2008).

The effect of electric field on interstitial transport of pDNA has been previously investigated by our lab and summarized in the works of Zaharoff and Henshaw. Electrophoretic movement of pDNA through the interstitium during pulsed, electric field was characterized in both ex-vivo and in-vivo tumor tissue and novel strategies to be used in tandem with EFMGD to enhance interstitial pDNA transport were investigated. This dissertation proceeds to investigate the effect of EFMGD in facilitating pDNA transport across the subsequent barriers of the cell membrane and the intracellular space. These next two physiological barriers were combined due to the common mechanism of endocytosis that governs DNA transport across them during EFMGD, as proposed by this dissertation.

In this dissertation, evidence obtained using different strategies will be presented to implicate multiple pathways of endocytosis in facilitating the internalization and intracellular trafficking of pDNA following pulsed, electric field treatment. Chapter 2 will provide background information regarding gene therapy as a promising treatment solution for a wide variety of diseases, the different types of non-viral gene therapy with emphasis on EFMGD, the fundamentals of EFMGD or electrotransfection, prior scientific

studies which have alluded to an active mode of pDNA uptake as a result of pulsed, electric field, and finally, the different endocytic pathways which could participate in pDNA internalization. Chapter 3 first investigates the effect of cation-mediated pDNA adsorption to cell membrane on the electrotransfection efficiency (eTE) of EFMGD. Trypsin treatment was then used to strip off membrane-bound pDNA at different timepoints after pulsed electric field and the effect on eTE was again noted. The results of these studies are used to refute electrophoresis, diffusion, and electro-osmosis as driving forces for pDNA transport across the cell membrane during EFMGD, thus indirectly implying the role of endocytosis in pDNA internalization. Pharmacological agents were used to transiently inhibit different endocytic pathways and their effects on eTE were determined. RNA interference using siRNA (small, interfering RNA) directed against dynamin II, a crucial endocytic GTPase protein associated with multiple endocytic pathways, was used as an alternate method of impairing endocytosis to determine the effect on eTE. In Chapter 4, the combination strategy of pharmacological inhibition and siRNA knockdown was again used to probe for and compare the specific endocytic pathways involved in electric-field mediated pDNA internalization in two additional cell lines. Finally, Chapter 5 will explore future studies and research directions in the field of electric field-mediated gene delivery. One proposed study entails utilizing fluorescent microscopy to observe the direct effect of endocytic inhibition on the internalization and intracellular distribution of fluorescently labeled

pDNA after pulse treatment, rather than noting their indirect impact on electrotransfection efficiency. Colocalization studies of fluorescently labeled endocytic vesicles with fluorescently tagged plasmid DNA is also proposed as an additional strategy for confirming endocytic uptake of pDNA following EFMGD. Finally, based on preliminary findings that are presented in greater detail in Chapter 5, it would be of interest to determine whether different pulsed electric field parameters recruit different endocytic pathways or combinations of pathways to facilitate pDNA uptake and intracellular trafficking within a cell line.

Chapter 2

BACKGROUND

2.1 Gene Delivery Approaches

Gene therapy is showing increasingly greater promise in the treatment of genetic diseases with advancements in molecular biology tools and increasing knowledge of the human genome. This approach of restoring normal, cellular function by introducing exogenous copies of healthy/therapeutic genes is hinged upon the successful delivery of plasmid DNA to the target cells/tissues and subsequent intracellular delivery to its final destination in the nucleus. A variety of delivery/carrier methods have been developed to facilitate the introduction of exogenous DNA into different cell systems and can be classified into two basic groups: viral and non-viral/synthetic vectors (Cristiano 1998; Cristiano, Xu et al. 1998; Robbins and Ghivizzani 1998; Strayer 1998). Viral delivery vehicles exploit the transduction abilities of retroviruses, adenoviruses, adeno-associated viruses and herpes simplex viruses to infect host cells with genes of interest. Viruses boasts the highest transfection efficiencies of all the different gene delivery methods, with adenoviruses, arguably the most efficient viral vector, generating transfection levels up to 90-100% in mice liver, human dendritic cells, and adult rat brain (Herz and Gerard 1993; Gerdes, Castro et al. 2000; Jenne, Schuler et al. 2001). Viral systems offer high

transfection efficiencies but suffer issues ranging from toxicity, immunogenicity, lack of target specificity, and high costs of production (Pack, Hoffman et al. 2005). Non-viral, chemical delivery vehicles mostly consist of synthetic vectors constructed of cationic lipids and polymers, which electrostatically bind polyanionic DNA into condensed complexes that shield the highly negative charge of DNA, facilitate cellular entry, and offer protection against nucleolytic enzymes. Whereas these synthetic vectors exhibit lower toxicity compared to recombinant viral carriers, they face their own challenges including poor transfection efficiency and instability *in vivo*.

Other non-viral alternative for gene delivery rely on various physical and mechanical means to facilitate DNA entry. Some of these methods include (Plank, Schillinger et al. 2003; Mehier-Humbert and Guy 2005):

- (i) Hydrodynamic gene delivery – the rapid injection of a large volume of naked plasmid DNA solution into circulation. In a mice model, this injection is administered at the tail vein, causing excessive fluid flow and pressure build-up in highly perfused organs, especially the liver. This method has resulted in transfection of 30-40% of the hepatocytes in the liver of treated mice (Liu, Song et al. 1999). Electron microscopy revealed the presence of transient, hydrodynamic treatment-induced membrane defects in these hepatocytes, which may potentially be the mechanism of DNA entry and transfection (Zhang, Gao et al. 2004). Although this method yields promising transfection results, there are

severe disadvantages that include significant cell and tissue damage, cell necrosis, and potential heart malfunction (Zhang, Vargo et al. 1997; Zhang, Budker et al. 1999), that makes it an unrealistic gene therapy strategy in humans.

- (ii) Particle bombardment (gene gun) – a ‘biolistic approach’ in which DNA is deposited onto the surface of heavy metal (gold or tungsten) microparticles of about 1-1.5 μm in diameter and accelerated into tissues and across the cell membrane into cells. DNA then gradually dissociates from the particles to transfect cells. The efficiency of this technique depends on factors such as the amount of DNA coated onto the particle surfaces, the microparticle sizes, the type of gun used (helium powered versus gun-powder; hand-held versus stand-alone), and the distribution of the DNA-coated beads within the tissue, which is affected by the acceleration rate generated by the gun. Transfection efficiencies of 30% have been achieved in cultured HEK293 (human embryonic kidney) cells (O'Brien and Lummis 2004) and in vivo expression levels of 20% have been seen in the bombarded area in mouse liver and skin tissue (Yang, Burkholder et al. 1990; Williams, Johnston et al. 1991). However, disadvantages of this technology include being reserved to only superficial, easily accessible tissues (e.g. skin), low DNA-loading capacity, and having limited depth of tissue penetration (less than 1 mm into skin) (Mehier-Humbert and Guy 2005).

(iii) Ultrasound-mediated gene delivery (Sonoporation) – application of focused ultrasound waves, resulting in formation of cavitation bubbles that induces biological effects such as microvascular hemorrhages and structural disruption of tissues, as well as cell death and transient membrane permeabilization on a cellular level (Miller, Pislaru et al. 2002). The collapse of these bubbles and the corresponding energy release destabilizes and permeabilizes cell membrane to facilitate cellular uptake of exogenous macromolecules and DNA into the cells. The transfection efficiency is affected by such parameters such as frequency, output strength magnitude, treatment duration, ambient temperature, and DNA and cell concentrations. In vitro gene expression levels are relatively low and range from < 1% for HeLa cells (Lauer, Burgelt et al. 1997) to 2.4% for primary rat fibroblasts (Kim, Greenleaf et al. 1996) to 20% for LnCap, a human prostate cancer cell line, (Tata, Dunn et al. 1997). However, addition of contrast agents, such as Albunex®, yielded substantially greater ultrasound-mediated transfection values of up to 43% in vitro (Greenleaf, Bolander et al. 1998). These agents are speculated to enhance transfection by acting as artificial cavitation nuclei to concentrate the number of cavitation events per unit volume and consequently, increase the number of cells affected by cavitation. In vivo transfection levels, however, remains low and hover below 5% (Miller, Bao et al. 1999; Huber and Pfisterer 2000).

- (v) Magnetofection - association of DNA and its viral or non-viral carriers with cationic magnetic nanoparticles made of biodegradable iron oxide with a polymer coating. These DNA-coated nanoparticles are then driven and concentrated within target cells by an external magnetic field. Magnetofection has achieved reasonable success in transfecting certain primary cell lines, endothelial cells, and difficult-to-transfect cells such as HUVECs (Scherer, Anton et al. 2002; Krotz, Sohn et al. 2003). Transfection efficiencies of up to 40% have been obtained in vitro for both HUVECs and porcine aortic endothelial cells when magnetic particles coated with PEI/DNA complexes were used (Scherer, Anton et al. 2002).
- (vi) Electroporation/Electropermeabilization – application of high voltage electric field pulses to induce transient, localized membrane permeabilization that permits the passage of DNA and other non-permeant macromolecules. Transfection efficiency of electroporation is highly dependent upon both physical (field magnitude, pulse duration, pulse number, pulse frequency, electrode configuration) and biological factors (DNA concentration, DNA configuration, cell density, cell size, pulsation buffer composition). These experimental factors must be empirically determined for each new cell line to optimize transfection efficiency. Electroporation has been used to transfect a variety of tissues and the efficiency of gene delivery in vitro ranges from 0.1% up to 55% (Toneguzzo,

Keating et al. 1988; Li, Chan et al. 1997; Bodwell, Swiff et al. 1999; Delteil, Teissie et al. 2000; Cemazar, Sersa et al. 2002). A method known as nucleofection (Amaxa Biosystems, Cologne, Germany), which combines electroporation with proprietary nucleofection solutions customized for a variety of cell lines, has been able to achieve extremely high, in vitro efficiencies of up to 95% without substantial costs to cell viability (Lakshmipathy, Pelacho et al. 2004; Nakashima, Matsuyama et al. 2005). Electroporation has also yielded promising in vivo results, with transfection efficiencies of 25-35% in embryonic chick hearts (Harrison, Byrne et al. 1998) and rat liver (Heller, Jaroszeski et al. 1996).

Of these aforementioned physical methods, electroporation remains to be one of the most widely used strategies for both in-vitro and in-vivo (Heller 1995; Heller, Ugen et al. 2005; Heller and Heller 2006; Heller, Jaroszeski et al. 2007) applications, due to its efficiency, simplicity of use, and safety (Escoffre, Portet et al. 2009).

2.2 Fundamentals of Electroporation

Since its introduction in 1982 by Neumann and colleagues (Neumann, Schaefer-Ridder et al. 1982) as an effective means of transfecting cells, electroporation has enjoyed widespread usage in biology and medicine yet little is still known about the mechanisms underlying electric-field induced membrane permeabilization (electropermeabilization),

DNA-membrane interaction during translocation, and the intracellular transport of DNA towards the nucleus.

2.2.1 Electroporation

Electroporation occurs when the application of an external, electric field pulse causes the transmembrane potential difference ΔV_m , of a cell to exceed a critical threshold value, ranging from 200 mV to 1V (Kinosita and Tsong 1977; Teissie and Rols 1993). To understand how an applied electric field induces permeabilization of the cell membrane, a cell can be represented as a simplified spherical, conductive body with a dielectric spherical shell as the plasma membrane that separates the intracellular and extracellular environment and maintains a resting transmembrane potential difference, ΔV_0 . When subjected to an electric field, an additional transmembrane potential difference, ΔV_E , is induced that varies in magnitude and direction depending on the position along the membrane with respect to the electric field. The electric field-induced change in transmembrane potential difference, ΔV_E , can be described by Equation 2.1.

$$\Delta V_E = -g(\lambda)rE \cos \theta(M)[1 - e^{-t/\tau}] \quad (2.1)$$

$$\Delta V_m = \Delta V_0 + \Delta V_E \quad (2.2)$$

$$g = \frac{2\lambda_i\lambda_e \frac{d}{a}}{\lambda_m(\lambda_i + 2\lambda_e) + 2\frac{d}{a}(\lambda_i - \lambda_m)(\lambda_e - \lambda_m)} \quad (2.3)$$

E is the externally applied electric field, r is the cell radius, θ is the angle between the direction of the E-field and a normal vector to point M on the membrane, t is the time after the onset of the electric pulse, and τ is the membrane charging time that depends on the dielectric properties of the membrane (Teissie, Golzio et al. 2005). g is a form factor that depends on the conductivities of the membrane λ_m , intracellular cytosol λ_i , and extracellular environment λ_e , as shown in Equation 2.3. The electric field-induced ΔV_E is added to the resting transmembrane potential difference ΔV_0 , typically -40 mV to -60 mV (Teissie, Golzio et al. 2005), to yield the net, position dependent ΔV_m (see Equation 2.2) that is hyperpolarized at the anode-facing pole and depolarized at the cathode-facing pole (Escoffre, Portet et al. 2009). When ΔV_m reaches its critical threshold (controlled by the applied E-field) at either poles facing the electrodes, the bilayer membrane at these regions undergo structural changes resulting in transient, increased permeability and rapid influx of non-permeant, extracellular molecules (Gehl 2003).

2.2.2 Transmembrane Transport of DNA

Entry of small molecules such as ions, dyes, radio tracers, and drugs into cells during electroporation has been shown to be a very rapid process that is driven by diffusion, electrophoresis, and/or electroosmosis (Golzio, Rols et al. 2004). Electrically-driven DNA transfer across the membrane, however, occurs on a much slower scale (order of minutes) (Golzio, Teissié et al. 2002) and precludes the aforementioned

transport modes as potential driving forces. Insight into its transmembrane transport can be gathered from studying the DNA-membrane interactions that take place at the permeabilized cell poles. The mechanism by which DNA interacts with electroporabilized membranes, resulting in DNA uptake is still uncertain, although several models have been proposed in the literature (Favard, Dean et al. 2007; Escoffre, Portet et al. 2009):

- (i) Formation of 'stable' electropores, estimated to be 20-200nm in diameter (Sugar and Neumann 1984; Krassowska and Filev 2007) during pulse duration that are large enough to permit free diffusion of locally-accumulated DNA into cell.
- (ii) Electrostatically-driven interactions with the polyanionic DNA and cationic sphingosine lipids causes DNA adsorption on cell surface. DNA is transiently inserted into the plasma bilayer and electrophoretically pulled through hydrophilic electroporated porous zones. (Spassova, Tsoneva et al. 1994; Hristova, Tsoneva et al. 1997)
- (iii) Electrophoretic forces push DNA through the putative electropores and mechanical interactions between the DNA and pore edges during passage dictate pore dynamics, size, and/or lifetime. (Kleinchin 1991; Sukharev 1992)

- (iv) DNA diffuses into the interior of the membrane bilayer, only after pore formation and completion of electric pulse, where the zwitterionic head groups of the lipids forms a stable complex with the DNA to facilitate its translocation across the membrane. (Tarek 2005)

Despite the aforementioned speculative models of pore formation during electroporation, these 'electropores' have never been visualized in living cells and their existence still remains to be confirmed (Teissie, Golzio et al. 2005). One study conducted by Chang et al., utilized rapid-freezing electron microscopy to capture formation of 'volcano-shaped membrane openings' on the membrane of red blood cells subjected to electric field (Chang and Reese 1990). Their findings, however, were later disputed as being an artifact resulting from the hypoosmotic extracellular conditions used.

The actual mechanism in which electric field then facilitates the translocation of DNA across the membrane is also uncertain and subject to much speculation. Such mechanisms as diffusion, electro-osmosis, and electrophoresis have been proposed (Michel, Elgizoli et al. 1988; Dimitrov and Sowers 1990), although electrophoresis has been suggested the most by several studies. Kleinchen et al. exhibited a 10-fold increase in transfection efficiency when electric field pulses were applied with a polarity inducing DNA electrophoresis towards a cell monolayer cultured on a porous film

versus pulses with reverse polarity. They also showed a 2-3 fold reduction in transfection efficiency when the electrophoretic mobility of DNA was reduced by either increasing the viscosity of the medium using 10% Ficoll or adding Mg^{2+} to reduce the effective charge of DNA (Kleinchin 1991). Electrophoresis was further suggested by the in vivo studies of Bureau et al., which demonstrated that transfection efficiency was significantly greater when a series of pulses, consisting of one high voltage, short pulse (to induce membrane permeabilization) followed by four low voltage, long pulses (to drive DNA electrophoresis), was used than when the single high voltage pulse or the four low voltage pulses alone were applied (Bureau, Gehl et al. 2000).

Experimental studies of DNA interactions with model lipid membranes and vesicles suggest alternate mechanisms of internalization. The work of Angelova and Tsoneva (Angelova, Hristova et al. 1999; Angelova and Tsoneva 1999) visualized DNA-induced endocytosis following DNA/lipid interaction and complex formation, when DNA molecules of varying sizes were locally microinjected near the surface of giant unilamellar vesicles (GUV). Proposed mechanisms for this phenomena suggest that local DNA/lipids interactions induce topological transformation of the bilayer that 1) *for small DNA fragments*, caused encapsulation of the DNA molecules within cylindrical inverted micellar domains along the membrane that were subsequently internalized as part of vesicles or 2) *for large DNA fragments*, caused membrane surface and charge asymmetries between the two lipid monolayers that were relieved by formation of

endosomes around the adsorbed DNA molecule(s). The formation of vesicles and endocytic uptake of high molecular weight DNA was also witnessed by Chernomordik et al., when GUVs were exposed to short, high-intensity pulses (12.5 kV/cm, 0.1-1ms) (Chernomordik, Sokolov et al. 1990).

Further insight into DNA/membrane interactions during electroporation can be gleaned from the visualization studies of Rols et al (Golzio, Teissié et al. 2002; Phez, Faurie et al. 2005). Using digitized fluorescence microscopy and YOYO-1 labeled plasmid DNA, they monitored the electrophoretically-driven accumulation of pDNA along the electropermeabilized, cell membrane sides facing the cathode. They witnessed the formation of discrete pDNA aggregates at numerous 'competent' membrane domains in this region when the field magnitude exceeded a critical threshold. These DNA clusters could not be eliminated when pulses of inverse polarity were applied, implying the formation of stable DNA-lipid complexes that could not be reversed. These aggregates were also susceptible to external DNA staining for up to 10 min after pulsing. After this time period, these DNA-lipid complexes were completely internalized and inaccessible to external dye. One can infer from these results that electric pulses contribute directly to 1) the induction of transient, permeabilized domains on the membrane surface 2) electrophoretic accumulation of polyanionic DNA along the interfacial membrane side facing the cathode, and 3) formation of stable DNA-membrane complexes at these membrane domains. However, actual translocation of

DNA across the membrane takes place over a prolonged period of time after the completion of pulsing, implying minimal/no effect from electric field but the potential involvement of cellular machinery/processes. Favard et al. (Favard, Dean et al. 2007) made the interesting observation that the size of these DNA-membrane aggregates/domains, ranging from 0.1-0.5 μm (Escoffre, Portet et al. 2009), were of the same order as lipid rafts. These sphingolipid- and cholesterol- enriched membrane domains serve as platforms to colocalize proteins involved in intracellular trafficking and signaling pathways (Calder and Yaqoob 2007) and may provide insight into the internalization and subsequent intracellular trafficking mechanism of electric field-mediated gene delivery.

2.3 Diffusion-negligible Intracellular Transport

It has long been believed that electroporation permits the influx of exogenous macromolecules such as pDNA from the extracellular environment directly into the cytosol. Once inside the cell, the pDNA relies on the simple yet purportedly effective means of diffusion through the aqueous cytoplasm to reach the nucleus, its targeted destination. While this may be satisfactory as applied to small solutes, several groups have presented evidence showing diffusion to be highly improbable as the dominant mode of transport for larger molecules such as pDNA. Lukacs et al. used fluorescence recovery after photobleaching (FRAP) to determine the diffusional mobilities of

fluorescently-labeled dsDNA of varying sizes that were directly microinjected into the cytoplasm. They determined the mobilities of DNA molecules in cytoplasm to be increasingly inhibited with increasing plasmid size compared to values measured in water: a ~ 17-fold decrease for sizes > 250 bp and over a 100-fold drop for fragments > 2000 bp (Lukacs, Haggie et al. 2000). pDNA of any therapeutic/functional capacity will minimally span a few kilobase pairs, thereby making it prohibitively inefficient for these molecules to rely on diffusion to transport them to the nucleus within a reasonable amount of time. Their hindered mobilities are most likely attributed to cytoplasmic crowding posed by the presence of various organelles, high protein concentrations, and the highly crosslinked network of the actin cytoskeleton (Favard, Dean et al. 2007). When cells were treated with different actin cytoskeleton disrupting/depolymerizing agents such as cytochalasin B, significant improvements were seen in their diffusional mobilities (Dauty and Verkman 2005). The cytosolic diffusional barrier is further exacerbated by the short half-life of naked pDNA in the cytosol, due to metabolic degradation by cytoplasmic nucleases. A 50% reduction in DNA in the cytoplasm was detected in 1-2 hours in HeLa and COS-1 cells (Lechardeur, Sohn et al. 1999) and as fast as 5 minutes in muscle cells (Bureau, Naimi et al. 2004).

Yet despite all of these cytoplasmic obstacles, significant reporter gene expression is achieved via electroporation and can be detected as soon as 4 hours after treatment (Haas, Jensen et al. 2002), which necessitates pDNA being successfully

transported to the nucleus. With diffusion ruled out as a feasible mechanism, the remaining alternative is directed, active transport. Active transport within the cytosol is carried out via different endocytic pathways that utilize a complex, intracellular microtubule network to transport cargo to designated locations such as the perinuclear region for nuclear entry or to lysosomes for degradation. The directed, deliberate transport of endocytic pathways would serve as a much more efficient and faster means of delivering the pDNA to the nucleus following electric field treatment.

Endocytosis has been shown to be the mechanism of uptake of various macromolecules following pulsed electric field treatment. Antov et al. demonstrated increased membrane adsorption of bovine serum albumin (BSA) and dextran molecules upon application of non-permeabilizing, low electric field (LEF) pulses via speculated electric-field induced changes in cell membrane composition, which consequently stimulated endocytic uptake of these molecules (Antov, Barbul et al. 2005). Rols et al. showed that the enzyme β -galactosidase was taken up by cells, even over an hour after electric field application, and was localized in large vesicles rather than being uniformly distributed throughout the cytoplasm. Post-pulse uptake of the enzyme was dramatically diminished when cells were pretreated with the macropinocytosis-inhibiting drug, colchicine, prior to pulsing (Rols, Femenia et al. 1995). Whether endocytosis is also responsible for DNA internalization following electric field treatment has, to the best of our knowledge, yet to be investigated.

2.4 Endocytic Pathways

Endocytosis, a ubiquitous process in all eukaryotic cells, is the regulated cellular internalization of extracellular ligands/proteins, membrane receptors, soluble molecules, etc., necessary for crucial cellular functions such as nutrient uptake, signal transduction, cell polarity generation, and general homeostasis (Mellman 1996; Conner and Schmid 2003). Many endocytic pathways exist within a cell to facilitate intracellular uptake of external macromolecules and to shuffle them from the plasma membrane to destinations throughout the cell, including the nucleus. These pathways all begin with the formation and budding of vesicles encapsulating external macromolecules (Khalil, Kogure et al. 2006), yet differ in the membrane composition which initiates the uptake, the nature of the cargo, the size of the vesicles generated, the mechanism of vesicle formation and trafficking, the regulatory proteins/molecules involved, and the intracellular fate of the macromolecules (Pouton, Wagstaff et al. 2007).

Endocytosis can be broadly classified into two categories: 1) Phagocytosis, the ingestion of large particles by specialized mammalian cells, such as macrophages, monocytes, and neutrophils (Conner and Schmid 2003), and 2) Pinocytosis, the uptake of fluid and solutes that occurs in all cell types (Vercauteren, Vandenbroucke et al. 2009). Although multiple different classification systems have been proposed to organize the many, different pinocytic pathways, one of the prevailing schemes further subdivides

pinocytosis into four general mechanisms: clathrin-mediated (CME), caveolae-mediated, macropinocytosis, and clathrin- and caveolae- independent endocytosis (**Figure 2.1**). Of these pinocytic pathways, clathrin- and caveolae- mediated endocytosis, along with macropinocytosis (Khalil, Kogure et al. 2006), have demonstrated roles in DNA uptake of different non-viral gene delivery vehicles (Rejman, Conese et al. 2006; Wong, Scales et al. 2007) . Since phagocytosis only occurs in specialized cells, it will not be discussed here. Clathrin- and caveolae- independent endocytosis will be touched upon briefly whereas the better characterized macropinocytic, clathrin-mediated, and caveolae-mediated pathways will be covered in greater depth.

2.4.1 Clathrin-mediated endocytosis

Clathrin-mediated endocytosis (CME) is the most well-characterized endocytic pathway and exists in all mammalian cells to perform critical functions such as regulation of signal transduction by controlling the membrane expression of signaling receptors and uptake of essential nutrients and growth factors such as cholesterol-carrying low density lipoprotein (LDL), iron-bound transferrin (Tfn), and epidermal growth factor (EGF) (Khalil, Kogure et al. 2006) .

Clathrin-mediated endocytosis (CME) is initiated upon binding of ligands to their specific transmembrane surface receptors, causing these ligand-receptor complexes to migrate towards and cluster within clathrin-coated pits (CCP) on the membrane. A

CCP complex is comprised of the assembly of three major proteins: clathrin, adaptor protein complex 2 (AP2), and dynamin. Clathrin is the main scaffolding protein with a triskelion (three-legged) structure composed of three heavy chains and three corresponding light chains, to form a polygonal lattice that facilitate membrane deformation/invagination and vesicle formation at these CCP sites. The AP2 complex is responsible for directing the formation and organization of the clathrin lattice, as well as mediating cargo selection and recruitment via different structural/functional domains. This heterotetrameric complex consists of four distinct subunits, each with unique functional roles. The α -adapting subunit identifies and targets the AP2 complex towards the sites of clathrin assembly on the membrane, the β -adapting subunit interacts with clathrin to direct its assembly, the μ 2-subunit interacts with internalization peptide motifs of cargo-bearing transmembrane receptors, and the σ 2-subunit serves to stabilize the whole assembly (Collins, McCoy et al. 2002; Conner and Schmid 2003). The GTPase dynamin facilitates scission of invaginated vesicles from the membrane for clathrin-mediated endocytosis, as well as caveolae-mediated and certain clathrin- and caveolae-independent pathways (Mayor and Pagano 2007) (Hinshaw 2000). This large molecule is recruited to invaginated clathrin-coated vesicles (CCVs) where it self-assembles to form spiral collars around the necks of CCVs. Upon GTP hydrolysis, dynamin proceeds to undergo conformational changes to generate pulling and/or twisting forces (Roux,

Uyhazi et al. 2006) (Sweitzer and Hinshaw 1998) that constricts the necks of CCVs, causing them to pinch off from the cell membrane.

Upon internalization, CCVs shed their clathrin coat to become early endosomes, which subsequently fuse with other endosomal vesicles, late endosomes and ultimately lysosomes for degradation (Doherty and McMahon 2009). Depending on the nature of the cargo within endosomes, its contents may alternatively be sorted to other intracellular destinations, such as the nucleus and Golgi apparatus or recycled back to the cell membrane (Khalil, Kogure et al. 2006).

2.4.2 Caveolae-mediated endocytosis

Caveolae are 50-80nm diameter flask-shaped invaginations of the plasma membrane at hydrophobic, detergent-resistant microdomains (commonly referred to as 'lipid rafts') on the cell surface that are enriched with cholesterol, glycosphingolipids, signaling proteins, and membrane transporters (Mayor and Pagano 2007). It is speculated that these rafts serves as a means of organizing and concentrating signaling molecules and membrane receptors to be internalized via similar endocytic pathways to similar intracellular destinations (Kurzchalia and Parton 1999). Caveolae-mediated endocytosis is one of several clathrin-independent pathways that associates/initiates at these lipid microdomains. Other raft domain-associated pathways are classified as clathrin- and caveolae- independent pathways and covered in the Section 2.4.4.

These membrane invaginations derive their name from the integral membrane protein caveolin that line their inner surfaces to establish their unique shape and structure. Caveolin-1, caveolin-2, and caveolin-3 (CAV1, CAV2, and CAV3, respectively) constitute the caveolin family of dimeric and multimeric proteins (Monier, Parton et al. 1995) that bind cholesterol and orient themselves along the plasma membrane with hydrophobic domains that embed within the inner membrane leaflet and both N- and C- termini protruding into the cytosol. Once aligned, they interlock with adjacent caveolins to form a protein coat around the caveolae (Conner and Schmid 2003).

Fluorescent caveolin 1-GFP fusion protein and FRAP (fluorescence recovery after photobleaching) studies (Thomsen, Roepstorff et al. 2002; Tagawa, Mezzacasa et al. 2005) have shown most of these caveolae structures to be relatively immobilized at the plasma membrane unless induced or stimulated (Parton, Joggerst et al. 1994; Sharma, Brown et al. 2004) to internalize, usually by ligand binding of receptors within the caveolae. One such ligand that is internalized almost exclusively by caveolae as its means of infection is simian virus 40 (SV40), making it an attractive tool for elucidating the intracellular processing and sorting of caveolae-dependent endocytosis (Chen and Norkin 1999; Pelkmans, Kartenbeck et al. 2001). Upon binding of this model substrate to multiple caveolae-associated membrane receptors, a signal cascade of events is initiated, which includes local cortical actin depolymerization, dynamin recruitment for vesicle

fission and formation of actin tails from the caveolae (Pelkmans, Puntener et al. 2002). This ultimately results in scission of the cargo-carrying caveolar vesicle from the cell membrane and migration into the cell. Depending on the nature of the cargo, the contents of the caveolar vesicle is subsequently sorted to early endosomes or to an intermediate intracellular organelle called a cavesome before arriving at their ultimate destinations at the endoplasmic reticulum (ER) or Golgi apparatus (Pelkmans and Helenius 2002; Pelkmans, Burli et al. 2004; Doherty and McMahon 2009). Cavesomes are structures exclusive to caveolar endocytosis, as they do not accrue ligand markers of other endocytic pathways (Kartenbeck, Stukenbrok et al. 1989; Pelkmans, Kartenbeck et al. 2001), and are distinguished by their caveolin-1 content, neutral pH, and glycosphingolipid- and cholesterol- rich membrane composition. Due to its neutral pH conditions, avoidance of a lysosomal degradative fate, and final destinations at the ER and Golgi complex, caveolae-dependent endocytosis is the preferred entry route for many viruses (Werling, Hope et al. 1999; Campbell, Crowe et al. 2001; Marjomaki, Pietiainen et al. 2002) and the targeted pathway for many gene delivery vehicles (Kirkham and Parton 2005).

2.4.3 Macropinocytosis

Macropinocytosis is a bulk-fluid and nonselective form of endocytosis that entails the formation of large vesicles of up to 5 μm in diameter (Swanson and Watts

1995) known as macropinosomes, usually at ruffling membrane domains. Certain cell types exhibit constitutive macropinocytosis whereas others only exhibit this activity upon stimulation by growth factors and other signals (Nichols and Lippincott-Schwartz 2001). This process is initiated by membrane ruffling, in which actin polymerization at certain sites along the cell membrane proceeds in a linear, radial fashion causing the outward projection of membrane protrusions. These protrusions will often recede back into the cytoplasm but may also collapse around a region of extracellular fluid and fuse with the plasma membrane around this region to form macropinosomes (Swanson and Watts 1995) (Doherty and McMahon 2009).

Unlike clathrin-mediated and caveolae-mediated endocytosis, macropinocytosis has no associated protein coat formation and does not concentrate membrane receptors, and much is still unknown about its regulatory process. However, it has been observed that macropinocytosis and membrane ruffles, occurs at unique membrane domains rich in cholesterol, glycosphingolipids, glycosyl phosphatidylinositol-linked proteins, and membrane proteins. Fission and internalization of macropinosomes do not require dynamin and the intracellular fate of these vesicles seem to depend on the cell type, leading to lysosomal degradation in macrophages (Meier and Greber 2003) and membrane recycling in human A431 cells (Swanson and Watts 1995). Macropinocytosis has been targeted as an attractive internalization route for gene delivery due to such advantageous characteristics as non-selective uptake of large macromolecules, a

relatively 'leaky' nature that is conducive to endosomal escape (Meier, Boucke et al. 2002; Wadia, Stan et al. 2004), and a non-degradative fate by avoiding the lysosomes.

2.4.4 Clathrin- and caveolae- independent endocytosis

Caveolae represents just one of several lipid microdomain-associated, clathrin-independent endocytic pathways. Caveolae- and clathrin- independent endocytosis is most likely composed of several different pathways that are both dynamin-dependent and -independent and which have been implicated in the internalization of extracellular fluid, cholera toxin B (CTxB), sphingolipids, GPI-linked proteins, and IL-2 (interleukin-2) receptors (Doherty and McMahon 2009). These pathways have been revealed by a process of exclusion in cells depleted of both clathrin- and caveolin- associated events and hence, are described only in negative terms (Conner and Schmid 2003; Doherty and McMahon 2009). Since these pathways have not yet all been discovered or well characterized, the mechanisms that govern vesicle formation, cargo recruitment, intracellular sorting and cellular destination for each of these pathways still remain poorly understood.

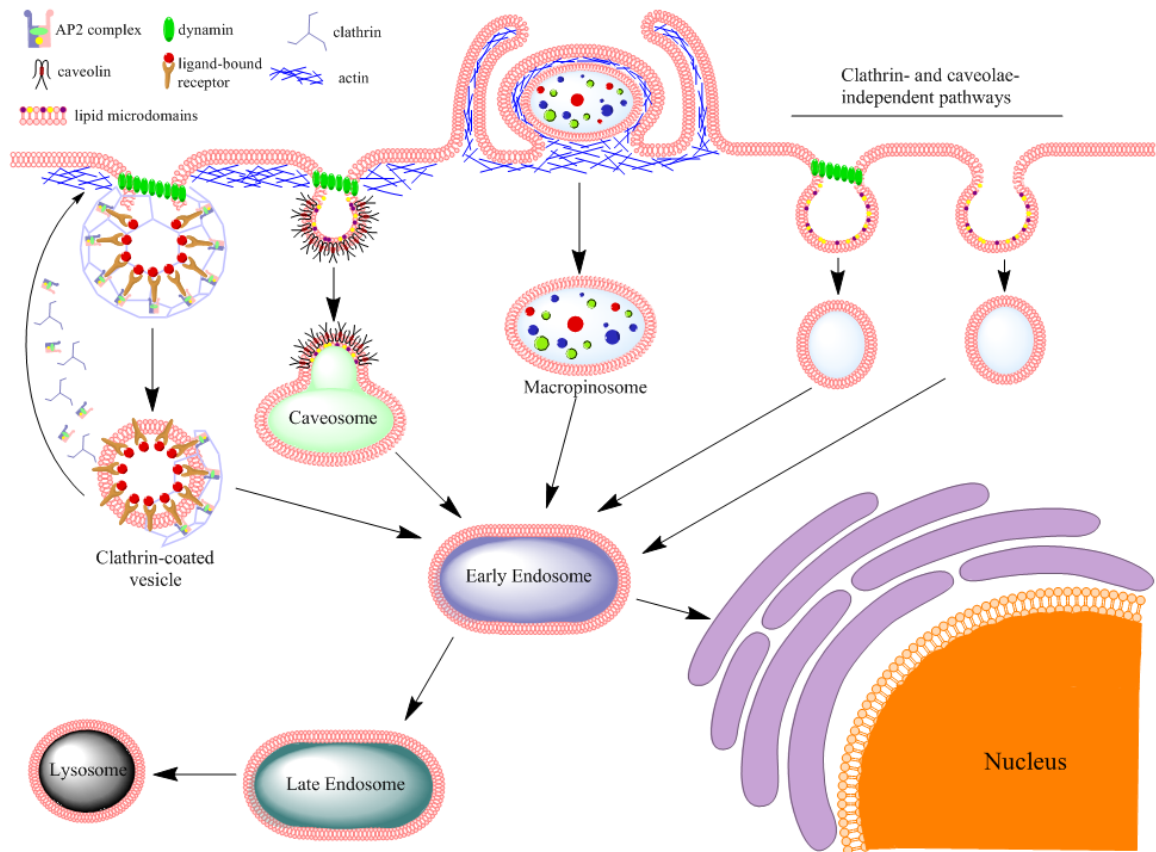


Figure 2.1: Pathways of endocytosis

Chapter 3

Membrane Binding of Plasmid DNA and Endocytic Pathways Are Involved in Electrotransfection of Mammalian Cells

3.1 Introduction

Pulsed electric field has been widely used for many years for improving gene delivery into cells both *in vitro* (Neumann, Schaefer-Ridder et al. 1982; Wolf, Rols et al. 1994) and *in vivo* (Heller, Jaroszeski et al. 1996; Nishi, Yoshizato et al. 1996; Aihara and Miyazaki 1998; Rols, Delteil et al. 1998; Mir, Bureau et al. 1999; Wells, Li et al. 2000; Lohr, Lo et al. 2001; Heller and Heller 2006). The technique is considered to rely on transient permeabilization of the plasma membrane of cells at hyperpolarized and depolarized poles facing the anode and cathode (Teissie, Golzio et al. 2005; Krassowska and Filev 2007), respectively, to allow polyanionic plasmid DNA (pDNA) to enter cells through permeabilized membrane facing the cathode. Several different terms have been used to describe the technique, including electroporation, electropermeabilization, electrogene transfer, gene electroinjection, and electrotransfection (Henshaw and Yuan 2008). These alternative terms are referred to as electrotransfection in this paper. Despite its numerous applications in biology, the main disadvantage of this technique, compared to

other gene delivery methods, is the difficulty in controlling its efficiency, which can vary by several orders of magnitude under different experimental conditions and electric field parameters. The optimization of cell transfection proceeds primarily by trial and error because of the poor understanding of the mechanisms governing electrotransfection.

It has been widely accepted that electrotransfection is dependent upon the phenomenon known as electroporation, whereby transient, hydrophilic pores are generated in the plasma membrane when the electric field-induced transmembrane potential difference exceeds a certain threshold level (200 - 1000 mV) (Weaver and Chizmadzhev 1996). Cell-impermeant molecules are then transported through these pores via mechanisms that may include diffusion (Michel, Elgizoli et al. 1988), electrophoresis (Mir, Bureau et al. 1999), and electroosmosis (Dimitrov and Sowers 1990). These mechanisms are likely to apply for delivery of small molecules but have yet to be shown to facilitate DNA transport across the membrane (Dimitrov and Sowers 1990; Weaver 1993; Prausnitz, Corbett et al. 1995; Bier, Hammer et al. 1999; Teissie, Golzio et al. 2005; Henshaw and Yuan 2008; Zaharoff, Henshaw et al. 2008; Haberl, Miklavcic et al. 2010). More recently, emerging evidence from various studies is challenging the “electroporation” mechanism for gene delivery (Faurie, Rebersek et al. ; Golzio, Teissié et al. 2002; Escoffre, Portet et al. 2009). Golzio *et al.* directly visualized electric field-mediated cell entry of pDNA in an *in vitro* study (Golzio, Teissié et al.

2002). Their observations in this and follow up studies demonstrate that applied electric field induces complex formation between pDNA and plasma membrane and that translocation of these pDNA complexes through the membrane occurs after, rather than during, electric pulse application (Faurie, Rebersek et al. ; Golzio, Teissié et al. 2002; Escoffre, Portet et al. 2009). The implication of these studies is that the applied electric field is necessary for electrophoretically pushing pDNA toward the cell membrane and for initiating complex formation between pDNA and the cell membrane, but that it may not be a driving force for pDNA entry into the cytosol. Therefore, the questions remain as to what are the mechanisms of pDNA internalization and how is it regulated by cells?

Another important observation in the literature is that DNA fragments of sizes comparable to pDNA are largely immobilized after direct injection into the cytosol (Lukacs, Haggie et al. 2000; Dauty and Verkman 2005), indicating that diffusion is highly improbable as a dominant mode of pDNA transport in the cytosol. The hindered diffusion has been attributed to cytoplasmic crowding posed by the presence of various organelles, high protein concentrations, and the highly cross-linked network of actin filaments (Favard, Dean et al. 2007). The cytosolic diffusional barrier is further exacerbated by the short half-life of naked pDNA, due to degradation by intracellular nucleases. The half-life of DNA in the cytosol is 1-2 hrs in HeLa and COS-1 cells (Lechardeur, Sohn et al. 1999) and only 5 min in muscle cells (Bureau, Naimi et al. 2004), suggesting that the time window for intracellular diffusion of intact pDNA is short. The

short time window and diffusional barriers imply that most internalized pDNA molecules cannot reach the nuclear envelope via diffusion (Vaughan and Dean 2006; Vaughan, Geiger et al. 2008). How, then, can electrotransfection achieve the high efficiencies observed in some studies? What are the mechanisms of intracellular transport?

To answer the questions raised above, we investigated the dynamics of electric field-induced pDNA interactions with the cell membrane and subsequent pDNA internalization and intracellular transport. Data from the study revealed that electrotransfection strongly relies upon (i) binding of pDNA to plasma membrane during electric field exposure and (ii) internalization of the membrane bound pDNA via endocytic-like processes.

3.2 Materials & Methods

3.2.1 Cell Culture

B16.F10, a murine melanoma cell line (Henshaw, Mossop et al. ; Henshaw, Zaharoff et al. 2007; Henshaw, Mossop et al. 2008), were cultured as monolayers in T75 flasks in high glucose Dulbecco's modified Eagle's medium (Invitrogen, Carlsbad, CA) supplemented with 10% bovine growth serum (Hyclone, Logan, UT) and penicillin/streptomycin (Invitrogen). The cells were incubated at 37°C in 5% CO₂ and

95% air and passaged every 2-3 days. For adsorption and electrotransfection experiments, 75-90% confluent T75 flasks were treated with 0.25% trypsin-EDTA (Invitrogen) for 5 min at 37°C, harvested by centrifugation, and washed with serum-containing medium to neutralize the activity of trypsin. Cells were then washed again with an electrotransfection buffer before final re-suspension in the same buffer at a concentration of $0.5-1 \times 10^7$ cells/ml. Two electrotransfection buffers were used in the study: 1) OptiMEM I Reduced Serum Media (Invitrogen, Carlsbad, CA) and 2) a low ionic strength medium (250 mM sucrose, 20 mM HEPES) supplemented with varying concentrations of calcium or magnesium ranging from 0.1 - 30 mM.

3.2.2 Plasmid

A 4.7 kbp plasmid (pEGFP-N1, Clontech, Palo Alto, CA), encoding enhanced green fluorescent protein (GFP), was amplified by transformed, Z-competent (Zymo Research, Orange, CA) DH5 α and Top10 *E. coli* strains and purified using the Qiagen Plasmid Maxi Prep Kit (Qiagen, Valencia, CA), as per manufacturers' protocols. For visualization and adsorption studies, the plasmid DNA (pDNA) was labeled with either YOYO-1, a DNA-intercalating fluorescence dye (Invitrogen), or LabelIT tetramethylrhodamine (TMR), which covalently bonds with DNA (Mirus Corp., Madison, WI). Depending on the concentration of pDNA, an appropriate volume of the 1 mM stock YOYO-1 solution was mixed with the pDNA solution to yield a basepair-to-

dye ratio of 5:1. The mixture was incubated at room temperature for at least 60 min prior to use. Covalent TMR labeling of the pDNA using the LabelIT kit was conducted as per manufacturer's protocol.

3.2.3 Membrane Adsorption of plasmid DNA

To study pDNA adsorption to the plasma membrane mediated by the cations (Ca^{2+} and Mg^{2+}), 3 μg of YOYO-1 labeled pDNA was added to 1 million B16-F10 cells suspended in 200 μL of the low ionic strength buffer with varying concentrations of Ca^{2+} or Mg^{2+} . The samples were incubated for 10 min on ice followed by 10 min at room temperature to simulate the electotransfection protocol without actual pulse application. Samples were then pelleted via centrifugation and re-suspended in 350-400 μL PBS without Ca^{2+} and Mg^{2+} . The percentage of cells that were associated with pDNA as well as the average fluorescence intensity of the same population of cells were quantified using flow cytometry.

3.2.4 Trypsin-Mediated Removal of Membrane-adsorbed DNA

To remove electric field-induced, membrane-adsorbed pDNA, B16-F10 cells were subjected to trypsin treatment following electrotransfection. In the experiment, cells were treated with 0.25% trypsin-EDTA for 30 min at 37°C, starting at 10 min post electrotransfection, which allowed cell recovery and electric field induced transient

pores in the membrane to re-seal at room temperature. Following the trypsin-EDTA treatment, the cells were washed with serum-rich DMEM to neutralize the trypsin, seeded in fresh serum-rich DMEM in 6-well plates, and incubated for 24 hrs. Flow cytometry was used to assess the effect of trypsin treatment on GFP expression.

3.2.5 Electrotransfection

1 million B16-F10 cells suspended in electrotransfection buffer (either OptiMEM or low ionic strength buffer supplemented with Ca^{2+} or Mg^{2+}) were mixed with 6 μg pEGFP-N1 to achieve a final sample volume of 100 μL . Samples were loaded into BTX disposable 4-mm gap aluminum cuvettes (Harvard Apparatus, Holliston, MA), and incubated on ice for 5-10 min before receiving an electric treatment of 8 pulses at 400 V/cm, 5 msec duration, and 1 Hz frequency. The pulses were generated by using BTX ECM 830 Square Wave Electroporation System (Harvard Apparatus). Samples were left in the cuvette for 10 min at room temperature post electrotransfection, to promote cell recovery and resealing of pores in the membrane. Then, the samples were spun down, decanted of electrotransfection buffer, and seeded in fresh serum-rich DMEM in 6-well plates. GFP expression was quantified using flow cytometry following 24 hrs of incubation.

To determine if the cations at varying concentrations could alter GFP expression, aside from mediating membrane adsorption of pDNA, 2 million B16-F10 cells were

mixed with 12 μg pEGFP-N1 in 200 μL of OptiMEM, incubated on ice for 5 min, and treated electrically using the same pulsing protocol as mentioned above. Samples were left in the cuvette for 20 min at room temperature to ensure complete resealing of pores in the membrane, spun down, and re-suspended in 200 μL of low ionic strength buffer of varying Ca^{2+} or Mg^{2+} concentrations. The cell suspensions were incubated on ice for 5 min, treated with the same electric field as above, and left in the cuvette for another 10 min at room temperature. Then, the cells were seeded in fresh serum-rich DMEM; and GFP expression in these cells was quantified after 24 hrs of incubation at 37°C.

3.2.6 Treatment of Cells with Pharmacological Inhibitors of Endocytosis

Stock solutions of the endocytic inhibiting drugs, chlorpromazine (CPZ), genistein, and dynasore (Sigma Aldrich, St. Louis, MO), were prepared in DMSO at concentrations of 5 mg/ml, 5 mg/ml, and 10 mg/ml, respectively, and stored at -20°C. $7-8 \times 10^5$ cells were seeded per well in a 6-well plate overnight to achieve 75-90% confluency in the following day. Media was aspirated and adherent cells were washed twice with PBS without Ca^{2+} and Mg^{2+} . 2 mL of serum-free DMEM was added to each well and appropriate volumes of the drugs were added to achieve final drug concentrations of 28 μM , 200 μM , and 80 μM for CPZ, genistein, and dynasore, respectively. In the control groups, equivalent volumes of DMSO without drugs were added into the wells. Cells were incubated with the drugs or DMSO at 37°C in 5% CO_2 and 95% air for 1 hr and

subsequently washed with PBS without Ca^{2+} and Mg^{2+} . Cells were trypsinized, washed again with serum-containing media, and re-suspended in OptiMEM at a density of 10^7 cell/mL. They were subsequently electrotransfected with pDNA encoding GFP to investigate effects of the drug treatment on electrotransfection efficiency.

3.2.7 Flow Cytometry

DMEM was aspirated from each well and adherent cells were washed twice with PBS without Ca^{2+} and Mg^{2+} . The cells were then detached by trypsinization, washed with serum-rich DMEM to neutralize trypsin activity, and resuspended in 350-400 μL of 5 $\mu\text{g}/\text{mL}$ propidium iodide (PI) in PBS. The BD FACScan flow cytometer (Becton Dickinson, Franklin Lakes, NJ), equipped with an argon laser with excitation wavelength of 488 nm and three fluorescent detectors (530/30, 585/42, 670LP), was used for simultaneous dual detection of GFP and PI fluorescence. Forward and side light scatterings were used as independent variables to exclude debris and isolate the cell population of interest. Compensation was set between 20-25% to resolve spectral emission overlap between the two channels and 10,000 events were collected for each sample. Autofluorescence from cells was corrected in each experimental group by using cell samples treated with the same protocol but in the absence of pDNA. BD CELLQUEST™ Software was used for data acquisition and analysis. The

electrotransfection efficiency was expressed as the percentage of total viable cells expressing GFP (PI negative, GFP positive).

3.2.8 Knockdown of Dynamin II Expression

B16-F10 cells were transfected with either of two specific Stealth small interfering RNA (siRNA) oligos (Invitrogen) directed against mouse dynamin II gene or the Stealth negative control siRNA (Medium GC) duplex (Invitrogen) using the Amaxa Nucleofector II System (Amaxa Biosystems, Cologne, Germany). The two siRNA oligos targeted the following sequences in the mouse dynamin II gene:

Sq1: 5'-GAGCCCGCATCAATCGTATCTTTCA-3'

Sq2: 5'-CATGAGCTGCTGGCTTACCTGTATT-3'

In the experiment, 1.5×10^6 cells were transfected with one of the siRNA oligos at a dose of 30 pmols using the Nucleofector Kit V (Amaxa) and Program P-020. The transfected cells were distributed evenly into 4 wells in a 6-well plate in order to achieve ~90% confluency after 48 hrs incubation. Cells were then harvested for Western blot analysis and pDNA electrotransfection experiment.

3.2.9 Western Blot Analysis

B16-F10 cells were subjected to siRNA treatment and pDNA electrotransfection in the same manner as described above, with the exception that all constituent

quantities/volumes were tripled for electrotransfection to ensure sufficient protein yield. Dynamin II expression levels were detected via immunoblot analysis after a 24-hr post-electrotransfection incubation period. Total protein content was isolated using a 10:1 mixture of CellLytic M Cell Lysis Reagent (Sigma Aldrich) to Protease inhibitor cocktail (Sigma Aldrich) and quantified using Pierce BCA Protein Assay Kit (Thermo Scientific, Rockford, IL). 10 µg of total protein extract per well was separated in a 7.5% Ready Gel Tris-HCl polyacrylamide gel (Bio-Rad, Hercules, CA), transferred onto PVDF membrane (Bio-Rad), blocked for 2-3 hours at room temperature in 5% milk, 20 mM Tris, 500 mM NaCl, 0.1% Tween20 (pH 7.5) and incubated overnight at 4°C with primary antibodies: mouse anti-dynamin 2 (B-2) (Santa Cruz Biotech, Santa Cruz, CA) and mouse anti-β-actin (C4) (Santa Cruz) as a loading control. Membrane was then probed with goat anti-mouse secondary antibody conjugated to horseradish peroxidase (Santa Cruz) for 45 min at room temperature, developed with SuperSignal West Pico Chemiluminescent Substrate (Thermo Scientific), and visualized with Amersham Hyperfilm™ ECL film (GE Healthcare, Buckinghamshire, UK).

3.2.10 Confocal Fluorescence Microscopy

All fluorescence images were acquired using the LSM510 confocal laser scanning microscope (Carl Zeiss, Thornwood, NY) and a 100X oil-immersion objective. Images shown in the figures represent optical slices near the middle plane of cells.

3.2.11 Statistical Analysis

Difference between experimental groups was compared using the Mann-Whitney U test. A difference was considered to be significant if the P value was < 0.05.

3.3 Results

3.3.1 Effects of divalent cations on pDNA adsorption to cell membrane and electrotransfection.

It has been reported that pulsed electric field induces complex formation between pDNA and cell membrane (Faurie, Rebersek et al. ; Golzio, Teissié et al. 2002; Escoffre, Portet et al. 2009). Although mechanisms of this complex formation are still unknown, we hypothesized that the process could be facilitated by divalent or multivalent cations that crosslink and, hence, anchor pDNA to negatively charged carbohydrates and proteins on the plasma membrane. To test this, we investigated the effects of divalent cations on pDNA binding to B16.F10 cell membrane, and quantified the dependence of pDNA adsorption on concentrations of Ca^{2+} and Mg^{2+} . In the study, fluorescently labeled pDNA was mixed with cells suspended in various cation-supplemented buffers and left to incubate for 20 min to promote adsorption, before flow cytometric analysis (for details see the Materials and Methods section). It was observed that the percentage of pDNA-associated cells was a nonlinear function of the

concentration for each cation (see **Figure 3.1A**), reaching a maximum value of ~16%. The average intensity of the pDNA-associated cells, on the other hand, increased approximately linearly with no sign of saturation when the concentration of each cation was increased (see **Figure 3.1B**).

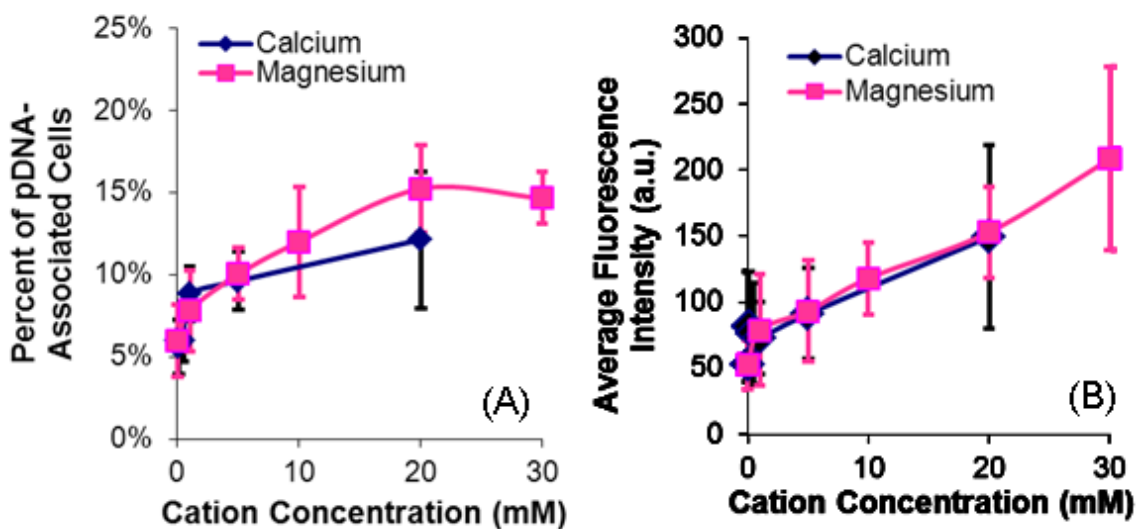


Figure 3.1: Dependence of membrane-bound pDNA on cation concentrations. pDNA was labeled with YOYO 1 dye with basepair-to-DNA ratio of 5:1. The binding was characterized in terms of (A) percent of pDNA-associated cells and (B) average fluorescence intensity with arbitrary unit (a.u.) per pDNA-associated cell. The number of independent trials (n) was 5-6. The symbols and error bars denote mean and standard deviation, respectively.

To investigate the consequent effects of this divalent cation-mediated pDNA adsorption on the delivery and electrotransfection of a reporter gene (i.e., green fluorescence protein (GFP)), the cells were incubated with pDNA for 10 min on ice to promote adsorption, followed by exposure to an electric field (8 pulses at 400V/cm, 5 msec duration, and 1 Hz frequency). After 24 hrs of incubation, electrotransfection

efficiency (eTE) was quantified using flow cytometry. The data shown in **Figure 3.2A** demonstrated that the eTE was enhanced by Ca^{2+} and Mg^{2+} at low concentrations but the enhancement was reduced when the concentrations were further increased. When no divalent cations were present in the low ionic strength buffer, the eTE was close to zero, suggesting that (a) cation-mediated pDNA adsorption was a necessary step for cell transfection and (b) electrophoresis of the polyanionic pDNA, which is inversely proportional to the ionic strength of a solution, does not play a critical role in electrotransfection, as suggested by some previous studies (Liu, Heston et al. 2006). To eliminate the possibility that the cation-dependent nature of eTE might be attributed to other cation-induced cellular effects aside from mediating pDNA-membrane interactions (i.e. changes in transcriptional and translational activities), a control experiment was performed in which cells were first electrotransfected with pDNA in OptiMEM. After a 20 min incubation period to permit sufficient membrane recovery, the cells were re-suspended in the low ionic strength buffer supplemented with cations at varying concentrations. The suspension was exposed again to the same electric field as before. The results shown in **Figures 3.2B** and **3.2C** demonstrated that when cations were not present during the actual pDNA electrotransfection but rather, introduced into the cells

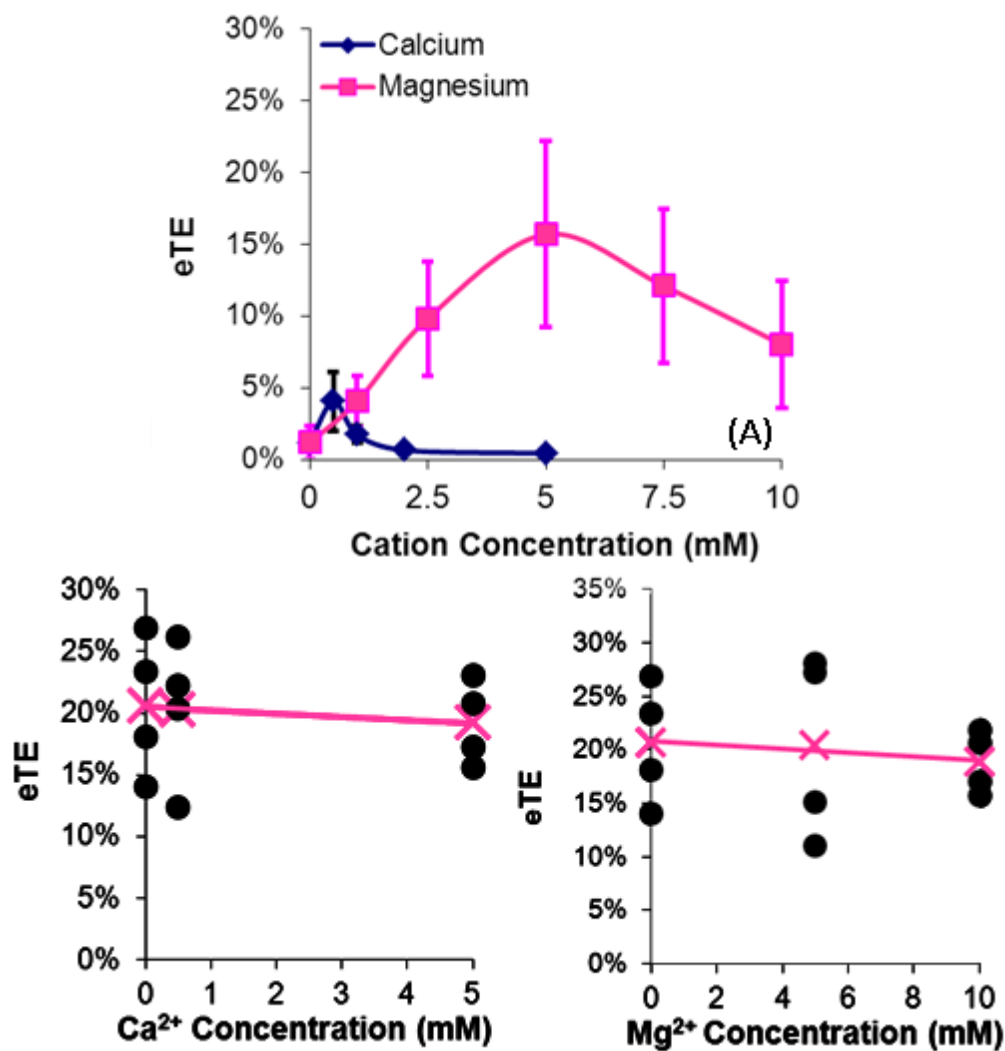


Figure 3.2: Dependence of electrotransfection efficiency on cation concentrations. eTE is defined as the percent of live cells expressing GFP. B16-F10 cells were electrotransfected (400 V/cm, 5 msec, 8 pulses, 1 Hz) with GFP-encoding unlabeled pDNA in a transfection buffer. (A) The low ionic strength medium supplemented with Ca²⁺ or Mg²⁺ at varying concentrations was used as the electrotransfection buffer. N = 7-8. The symbols and error bars denote mean and standard deviation, respectively. The peak eTE value in each curve was significantly higher than those at both ends of the same curve ($P < 0.05$). In Panels (B) and (C), OptiMEM was used as the electrotransfection buffer. After 20 min incubation post electrotransfection, the cells were re-suspended in the low ionic strength medium supplemented with either Ca²⁺ or Mg²⁺ at varying concentrations, and treated again with the same electric field. The GFP expression was quantified at 24 hrs. n = 4. The filled circles denote data from individual samples, the “x” symbol represents the mean of the samples at a given cation concentration, and the line represents the linear regression of the mean data. The mean value was statistically independent of the variation in Ca²⁺ and Mg²⁺ concentrations ($P > 0.05$, Mann Whitney U test).

in the presence of electric field 20 min later, the varying cation concentrations did not produce statistically significant changes in eTE, suggesting that Ca^{2+} and Mg^{2+} had minimal effects on normal transcriptional and translational function in treated cells.

3.3.2 Slow internalization of pDNA after exposure to electric field.

Previous studies have shown that eTE can be significantly reduced in bacterial and Chinese hamster ovary (CHO) cells if they are treated with DNase within a few seconds or ~ 1 min, respectively, of pulsed electric field application (Eynard, Rols et al. 1997). The observation suggests that, at these timepoints, either the cell membrane was still permeable to DNase resulting in the degradation of internalized pDNA, or a large fraction of pDNA molecules were not internalized shortly after electric field treatment. To investigate when pDNA internalization is fully completed, we treated cells with DNase (10 U per μg pDNA for 30 min at 37°C) to digest extracellular YOYO 1-labeled pDNA or trypsin (0.25% for 30 min at 37°C) to cleave DNA-bound proteins associated with the membrane, at 10 or 40 min after electric field application. The DNase treatment was inadequate in digesting membrane-bound pDNA, as determined by fluorescence microscopy. However, pDNA bound to the membrane could be effectively removed by trypsin (see **Figure 3.3A&B**). Trypsin treatment was seen to significantly reduce eTE if administered at 10 min but had no effect at 40 min, when compared to the control (i.e.,

no trypsin case) (see **Figure 3.3C**), suggesting that the internalization of membrane-bound pDNA was completed between 10 and 40 min after electric field application.

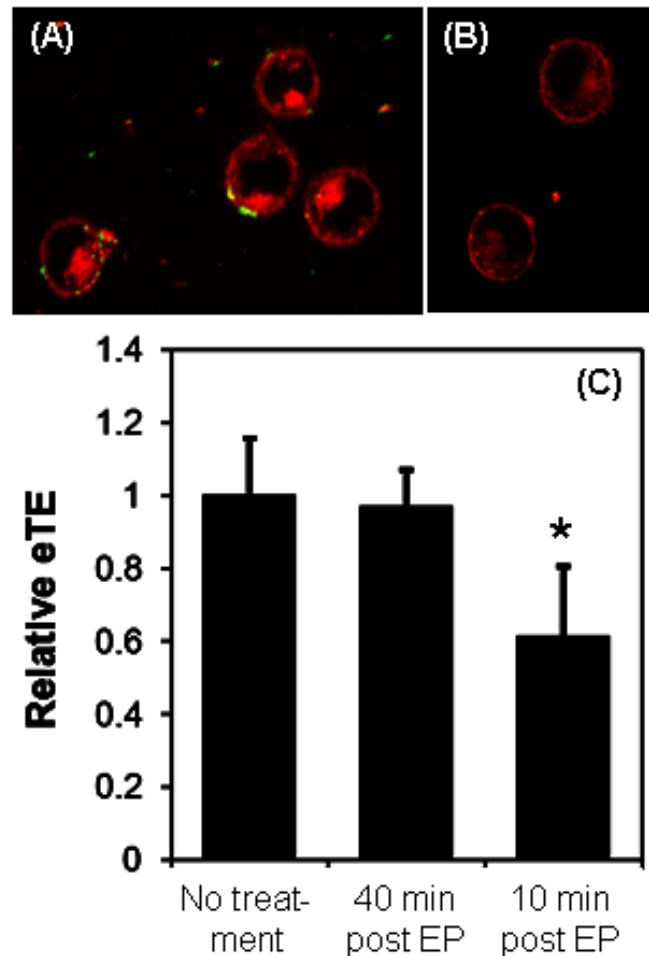


Figure 3.3: Effects of trypsin treatment on pDNA adsorption to cell membrane and eTE. (A) YOYO 1-labeled pDNA (green) formed complexes with FM4-64FX labeled plasma membrane (red) following exposure of cells to pulsed electric field (400 V/cm, 5 msec, 8 pulses, 1 Hz). The image was taken shortly after the application of electric field. (B) The experimental protocol was the same as that in the Panel (A), except that at 10 min post electric field exposure, the cells were treated with 0.25% trypsin-EDTA solution for 30 min at 37°C. The image was taken after the trypsin treatment. (C) B16-F10 cells in pDNA solution were exposed to the same electric pulses (EP) as above. At 10 or 40 min post EP exposure, the cells were treated with 0.25% trypsin for 30 min at 37°C. Then, the cells were cultured for 24 hrs at 37°C. The eTE was measured as the percent of live cells expressing GFP and normalized by the data from the no treatment group. The solid column and error bar represent mean and standard deviation of the relative eTE, respectively. n = 6 - 9. * P < 0.05 (Mann-Whitney U test).

3.3.3 Effects of endocytic inhibitors on electrotransfection efficiency.

Three pharmacological inhibitors of endocytosis were used in the study: chlorpromazine (CPZ), genistein, and dynasore, which block clathrin-coated pit formation, caveolae-mediated endocytosis, and dynamin activity, respectively (Rejman, Bragonzi et al. 2005; van der Aa, Huth et al. 2007; Gratton, Ropp et al. 2008). Dynamin, a GTPase involved in clathrin-mediated as well as certain clathrin-independent endocytosis, facilitates fission of vesicles from the plasma membrane, resulting in release of the vesicles into the cytosol (Doherty and McMahon 2009). In the first experiment, B16.F10 cells were treated with dynasore or the drug vehicle DMSO (control) for 1 hr prior to electrotransfection with rhodamine-labeled pDNA. After electrotransfection, cells were incubated at 37°C for 30 min and the internalized pDNA molecules were visualized using confocal microscopy. **Figures 3.4A through 3.4C** demonstrated qualitatively that dynasore treatment could reduce the uptake and intracellular distribution of electrotransfected pDNA in cells. In the second experiment, B16.F10 cells were pre-treated with each of the pharmacological inhibitors for 1 hr followed by electrotransfection with unlabeled pDNA encoding GFP. The eTE was quantified after 24 hrs of incubation. The data shown in **Figure 3.4D** demonstrated that all three pharmacological inhibitors could significantly reduce eTE ($P < 0.05$), compared to the control group, in which the cells were treated with equivalent volumes of DMSO alone.

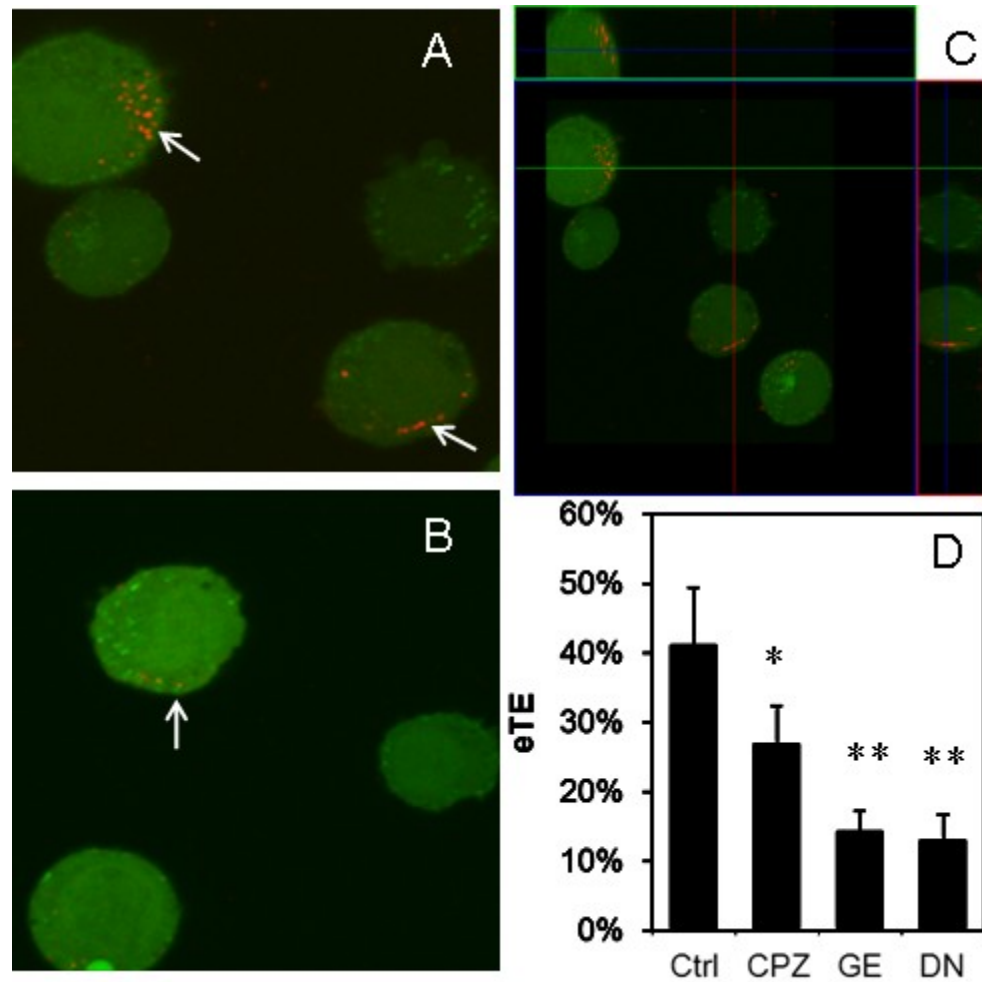


Figure 3.4: Reduction in cellular uptake of pDNA and the eTE by endocytic inhibitor treatment. pDNA covalently labeled with rhodamine (red) was electrotransfected (400 V/cm, 5 msec, 8 pulses, 1 Hz) into cells pre-treated with (A) DMSO (drug vehicle) or (B) dynasore (80 μ M) for 1 hr. After electrotransfection, the cells were incubated at 37°C to enable cellular uptake of pDNA for 30 min. At the end of incubation, the cells were examined using confocal microscopy. Arrows in the microscopic images denote pDNA internalized by cells. To visualize three-dimensional distribution of pDNA in the cytosol, two optical cross-sections of DMSO-treated cells in x-z and y-z planes are shown in Panel (C). Effects of endocytic inhibitor treatment on the eTE are shown in Panel (D). Cells were treated with DMSO (Ctrl), 28 μ M CPZ, 200 μ M genistein (GE), or 80 μ M dynasore (DN) for 1 hr prior to electrotransfection with the GFP-encoding pDNA. The eTE, defined as the percent of live cells expressing GFP, was quantified after cells were cultured at 37°C for 24 hrs. n = 4 - 6. * P < 0.05 and ** P < 0.005 (Mann-Whitney U test).

3.3.4 Dependence of electrotransfection efficiency on dynamin expression.

B16-F10 cells were treated with either of two specific, small interfering RNA (siRNA) sequences directed against two different sequences in the mouse dynamin II gene (i.e., Sq1 and Sq2 described in the Materials and Methods section) or a negative control siRNA sequence with similar GC content. Western blot analysis revealed that only siRNA sequence Sq1 resulted in sustained silencing of dynamin II expression (see **Figure 3.5A**) during the entire experimental period. The effects of dynamin II silencing on eTE using GFP-encoding pDNA are shown in **Figure 3.5B**. Cells treated with siRNA sequence Sq1 had significantly lower eTE than the control siRNA-treated cells ($P < 0.05$). However, there was no statistically significant difference in eTE ($P = 0.19$) between cells treated with siRNA sequence Sq2 and the control siRNA. These data demonstrates that specific knockdown of dynamin II expression directly result in a ~50% reduction in eTE.

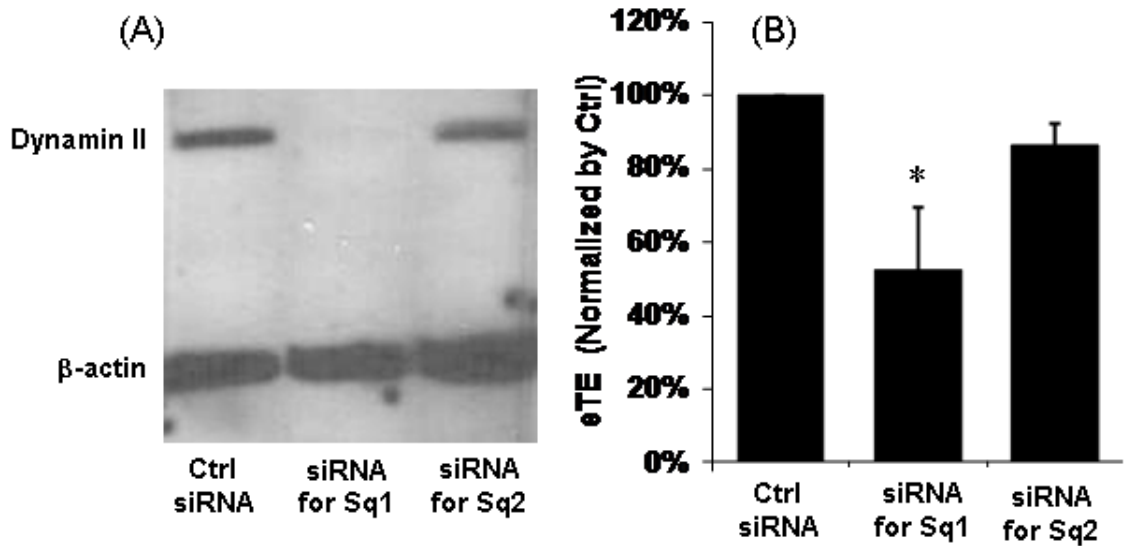


Figure 3.5: Effects of dynamin II knockdown on pDNA electrotransfection. B16-F10 cells were transfected with either the control siRNA or one of the two specific siRNA oligos directed against two different sequences (i.e., Sq1 and Sq2) in mouse dynamin II gene for silencing its expression. The siRNA treatment was followed by pDNA electrotransfection with a 48-hr delay. Dynamin II and β-actin (loading control) expression levels in Western blot analysis are shown in Panel A and normalized electrotransfection efficiencies are shown in Panel B. The bars and error bars indicate the means and standard deviations of 4 independent trials, respectively. The data from each trial, used in mean and standard deviation calculation, was the average value of replicates or triplicates. *, $P < 0.05$ (Mann-Whitney U test).

3.4 Discussion

Data in this study showed that Ca^{2+} and Mg^{2+} could facilitate pDNA adsorption to the cell membrane. There existed optimal concentrations of Mg^{2+} at which the percentages of pDNA-associated cells and GFP-expressing cells, respectively, reached their maximum levels even though the average concentration of membrane-bound pDNA in these cells increased linearly with increasing Mg^{2+} concentration. Furthermore, the eTE could be reduced by trypsinization of cells at 10 min post electrotransfection or

treatment of cells with (i) pharmacological inhibitors for endocytosis or (ii) anti-dynamin II siRNA prior to electrotransfection. These observations demonstrated that electric field mediated cellular uptake of pDNA is a slow process relative to the half-life of transient electropores induced in the membrane, that it must be preceded by binding of the pDNA to the plasma membrane, and that it is highly dependent on specific molecules implicated in endocytic vesicle formation.

3.4.1 Effects of cations on pDNA delivery

Divalent cations can affect pDNA transport into cells and electrotransfection efficiency through in multiple, different ways. First, the cations can function as bridges that crosslink the polyanionic DNA and negatively charged carbohydrates and proteins associated with the plasma membrane of cells (Neumann, Schaefer-Ridder et al. 1982; Xie and Tsong 1993; Frantescu, Tonsing et al. 2006; Mengistu, Bohinc et al. 2009; Haberl, Miklavcic et al. 2010). Ca^{2+} has also been shown to form ternary complexes with DNA and negatively charged lipids in unilamellar liposomes (Frantescu, Tonsing et al. 2006). The amount of DNA adsorbed on the lipid membrane increases with increasing concentration of cations (Xie and Tsong 1993). In our study, the percentage of pDNA-associated cells was < 16% (see **Figure 3.1A**) whereas the amount of pDNA adsorbed to these cells increased linearly with increasing concentration of cations (see **Figure 3.1B**). This suggested that the membrane-associated carbohydrates and proteins in >80% of the

cells might have been thoroughly stripped off by the trypsin treatment required to generate single-cell suspensions in the study. Therefore, few pDNA molecules could adsorb to the majority of cells. Another observation shown in **Figure 3.1** was that the amount of pDNA adsorbed on the membrane was low but not zero when no divalent cations were present, suggesting that non-specific binding between pDNA and the membrane was present, albeit weak. It should be pointed out that pDNA adsorption to the membrane via divalent cations differs from the complex formation between pDNA and the membrane discovered in previous studies (Faurie, Rebersek et al. ; Golzio, Teissié et al. 2002; Phez, Faurie et al. 2005; Escoffre, Portet et al. 2009). The latter is induced by pulsed electric field whereas the former is field-independent. However, the adsorption can enhance complex formation by increasing the local concentration of pDNA next to the cell membrane.

Second, divalent cations in the electrotransfection buffer can bind to pDNA to neutralize its charge and cause DNA aggregation (Duguid, Bloomfield et al. 1993). The neutralization will reduce the driving force for electrophoresis during electrotransfection, thereby reducing pDNA transport from extracellular medium into cells. At higher concentrations, divalent cations could cause pDNA aggregation by cross-linking multiple DNA molecules. Both neutralization and aggregation can reduce the eTE since less pDNA molecules will be delivered into cells. These phenomena may explain the trend observed in some previous studies where eTE decreases with

increasing concentration of Mg^{2+} (Neumann, Schaefer-Ridder et al. 1982; Haberl, Miklavcic et al. 2010). However, our data shown in **Figure 3.2A** differed from these studies, in that the eTE exhibited a bell-shape dependence on both the Ca^{2+} and Mg^{2+} concentrations. Our data were similar to the results reported in another study (Xie and Tsong 1993). The discrepancy between these studies could be caused by differences in experimental design. In the study by Haberl et al. (Haberl, Miklavcic et al. 2010), pDNA was added into the electrotransfection buffer (40 μ g/ml), containing cells (2.5×10^6 per ml) and Mg^{2+} , within 2-3 min before pulsed electric field treatment. In our study, the pDNA concentration was 50% higher, the cell density was 4 times higher, and pDNA was added into the buffer at 5-10 min before electric field application. The increase in both pDNA concentration and cell density reduced the average distance between pDNA and cells. With the shorter diffusion distance and longer diffusion time, our protocol allowed more pDNA molecules to be adsorbed on the membrane before electrotransfection. As a result, pDNA delivery towards cells was less reliant on electrophoresis during electrotransfection since a significant fraction of pDNA molecules were already bound to the membrane before exposure to electric field (Xie and Tsong 1993). However, higher cation concentrations may also cause such strong pDNA-membrane binding that pDNA remains anchored to the membrane after electric field application and is, thus, unable to enter the cell for GFP expression (Haberl, Miklavcic et al. 2010). The pDNA immobilization might be one of the factors contributing to the decrease in eTE observed

in **Figure 3.2A** when Ca^{2+} or Mg^{2+} concentration exceeded a threshold level. It should be noted that the low ionic strength buffer supplemented with Ca^{2+} or Mg^{2+} was not optimized for electrotransfection since it contained only one cation, Ca^{2+} or Mg^{2+} . On the other hand, OptiMEM likely contains several multivalent cations and other charged species that could enhance the binding of DNA to the cell membrane although the exact formulation of OptiMEM is unknown due to its proprietary nature. The differences in cation species and their concentrations may explain why the peak levels of eTE in our buffer were lower than the average eTE in OptiMEM (see **Figure 3.2**). It is expected that the new mechanisms of electrotransfection revealed in this study may lead to development of new, optimized buffers that may outperform OptiMEM in terms of eTE.

Third, it is well known that Ca^{2+} and Mg^{2+} can enhance exocytosis, endocytosis, and vesicle recycling (Williams and Wagner 1981; Artalejo, Henley et al. 1995; Zefirov, Abdrakhmanov et al. 2006; Hay 2007; Doherty and McMahon 2009), which are often coupled together in cells. Extracellular concentrations of these cations used in the previous studies vary between 1 and 10 mM (Williams and Wagner 1981; Artalejo, Henley et al. 1995; Zefirov, Abdrakhmanov et al. 2006), which were similar to the concentrations used in our study. Fourth, endonuclease activity can be enhanced by divalent cations at 1 mM concentration (Lechardeur, Sohn et al. 1999), which may reduce the half-life of DNA in cells. However, this effect is negligible in our study as shown by the data in **Figures 3.2B** and **3.2C**, in which cations delivered into cells shortly after

electrotransfection had minimal effects on the eTE. In summary, data in the literature and our study suggested that Ca^{2+} and Mg^{2+} could potentially affect pDNA transport into cells and the eTE by facilitating pDNA binding to cell membrane and enhancing endocytosis of membrane-bound pDNA.

3.4.2 Effects of adsorbed pDNA on membrane surfaces

A flexible membrane is required for invagination and internalization of bound pDNA molecules. There is evidence that pDNA adsorption may decrease membrane stiffness and cause structural changes in the membrane. When small DNA fragments (~300 bp) are adsorbed to the membrane of unilamellar vesicles via Ca^{2+} , the membrane stiffness is decreased, which reduces the energy barrier to electroporation (Francescu, Kakorin et al. 2005). Similarly, large T7 DNA and pDNA molecules adsorbed onto lipid membrane through divalent cations can induce formation of DNA-containing endosome-like vesicles in unilamellar liposomes (Chernomordik, Sokolov et al. 1990). The liposomal uptake of large DNA can be further enhanced by applying pulsed electric field (Chernomordik, Sokolov et al. 1990). The same structural changes might also occur in the plasma membrane of living cells to facilitate the endocytosis of pDNA proposed in our study, although further investigation is required to demonstrate these changes directly.

3.4.3 Dynamics of pDNA internalization after exposure to electric field

DNA visualization studies demonstrate the formation of both metastable and stable complexes between pDNA and the region of the plasma membrane facing the cathode, when the field magnitude exceeds a critical threshold (Faurie, Rebersek et al. ; Golzio, Teissié et al. 2002; Phez, Faurie et al. 2005; Escoffre, Portet et al. 2009). It is the stable form of these complexes, which cannot be eliminated by reversing the polarity of the electric field, that determines the efficiency of gene delivery. pDNA molecules in the complex are susceptible to external staining with TOTO-1 dye at 1 sec after pulsing but become inaccessible to TOTO-1 at 10 min (Golzio, Teissié et al. 2002). In another study, the pDNA molecules are accessible to external DNase within 1 min after the application of electric field (Eynard, Rols et al. 1997). These findings, albeit important, do not clearly determine the location of the pDNA complexes as being inside the cell, within the membrane, or on the extracellular side of the membrane since the lack of fluorescence staining or pDNA degradation may be attributed to an inability of TOTO-1 or DNase to penetrate the complexes and access their target DNA sites. Data in this study suggested that a significant fraction of the pDNA complexes were still on the outer surface of the membrane at 10 min post electrotransfection since trypsinization of cells could reduce the eTE (see **Figure 3.3**). At 40 min following electrotransfection, trypsinization had no effects on the eTE, suggesting that the process of cellular uptake of pDNA was finished completely between 10 and 40 min, which greatly exceeds the lifetime (~ 10 msec) of the

transient membrane pores induced by electric field (Krassowska and Filev 2007). This data implies that a large fraction of pDNA molecules entered the cells after the pores had resealed, which precludes diffusion and electrophoresis from playing important roles in transmembrane transport of pDNA molecules.

3.4.4 Effects of endocytic impairment on electrotransfection efficiency

In this study, we demonstrated statistically significant reductions in the eTE induced by different pharmacological inhibitors of endocytosis (i.e., chlorpromazine, genistein, and dynasore) (see **Figure 3.4D**). It was also observed in **Figure 3.4A-C** that dynasore substantially reduced the intracellular distribution of rhodamine-labeled pDNA following electric field treatment, which explains the corresponding reduction in eTE shown in **Figure 3.4D**. These findings are further substantiated by the siRNA silencing experiment which show a substantial reduction in eTE as a direct result of dynamin II knockdown (**Figure 3.5**). These data together strongly suggested that electric field mediated-pDNA uptake and intracellular transport relied, in some capacity, on endocytic pathways and vesicle trafficking mechanisms. Further investigations are required to understand the specific endocytic pathways and mechanisms involved.

Several previous studies have speculated upon or presented indirect evidence of the potential role of endocytosis in electrotransfection. For example, it is energetically feasible for the applied electric field to induce membrane invagination during

electrotransformation (Sabelnikov 1994; Neumann, Kakorin et al. 1996). Pulsed electric field has been observed to enhance liposomal uptake of membrane bound DNA into endosome-like vesicles (Chernomordik, Sokolov et al. 1990). For mammalian cells, Favard *et al.* have observed the size of these electric field induced pDNA-membrane complexes to be on the same order of magnitude as that of lipid rafts (Favard, Dean et al. 2007; Escoffre, Portet et al. 2009), which are plasma membrane microdomains enriched in cholesterol and sphingolipids that are involved in raft-dependent endocytosis (Nabi and Le 2003; Pike 2004; Kirkham and Parton 2005; Khalil, Kogure et al. 2006). Direct measurements showed that pulsed electric field could stimulate endocytosis of fluorescein-label bovine serum albumin (Glogauer, Lee et al. 1993; Antov, Barbul et al. 2005) and β -galactosidase (Rols, Femenia et al. 1995).

A seemingly contradictory study was conducted by Pavlin *et al.*, in which the authors observed that both high and low electric field could lead to vesicle formation within mammalian cells but only high electric field would result in successful gene delivery (Pavlin, Kanduser et al. 2009). Thus, the authors concluded that endocytosis of pDNA was not involved in electrotransfection and suggested that the vesicles induced by the applied electric field were related to exocytosis that was triggered for repairing electrically-damaged membrane. However, an alternative explanation for the same observation exists. The endosome-like vesicle formation has been observed in unilamellar liposomes when liposomes in the DNA solution are exposed to pulsed

electric field (Chernomordik, Sokolov et al. 1990). In this case, there is no exocytosis. The vesicle formation results in DNA uptake by liposomes and the amount of uptake increases with increasing electric field strength (Chernomordik, Sokolov et al. 1990). Furthermore, it has been shown that DNA-membrane complex formation is a necessary step for electrotransfection and that complex formation occurs only if the field magnitude exceeds a threshold (Faurie, Rebersek et al. ; Golzio, Teissié et al. 2002; Phez, Faurie et al. 2005; Escoffre, Portet et al. 2009). Therefore, the lack of cell transfection at low electric field observed by Pavlin *et al.* could be due to the inability for pDNA molecules to form stable complexes with the cell membrane.

3.5 Conclusions

It has become a widely accepted, yet poorly proven hypothesis that electroporation delivers macromolecules, regardless of their nature, directly into the cytosol via diffusion and/or electrophoresis through transient pores created by pulsed electric field. The findings in this study offer the first compelling, direct evidence to support an alternative hypothesis that electric field-mediated internalization of pDNA is dependent upon endocytic pathways. Data in this study show that (a) the internalization process was several orders of magnitude longer than the known lifetime of transient pores induced by electric field, (b) pDNA adsorption to the plasma membrane was a necessary step for cellular uptake during electrotransfection, and (c) both cellular uptake

of pDNA and transgene expression could be reduced by using well-established endocytic inhibitors and anti-dynamin II siRNA (Rejman, Bragonzi et al. 2005; van der Aa, Huth et al. 2007; Gratton, Ropp et al. 2008). The endocytosis can be triggered by pulsed electric field both directly (Chernomordik, Sokolov et al. 1990; Glogauer, Lee et al. 1993; Rols, Femenia et al. 1995; Satkauskas, Bureau et al. 2001; Antov, Barbul et al. 2005) and indirectly through inducing the formation of pDNA-membrane complexes (Faurie, Rebersek et al. ; Golzio, Teissié et al. 2002; Escoffre, Portet et al. 2009). Specific pathways of pDNA endocytosis remain unknown and will need to be investigated in future studies. An understanding of these pathways will allow scientists to develop novel strategies for improving the efficiencies of cell transfection and gene manipulation. They may also reveal new information for addressing fundamental questions in cell biology and biophysics.

Chapter 4

Endocytic Pathways are Recruited for Electric Field-mediated DNA Uptake in a Cell-dependent Manner

4.1 Introduction

Effective cell transfection using pulsed, electric field is hinged upon overcoming a series of major physiological barriers from the origin site of DNA administration to its ultimate destination in the nucleus of the target cells (Henshaw and Yuan 2008). Two of the major barriers encountered are the cell membrane and the intracellular environment, which pose physical, biological, and chemical obstacles to DNA transport. The mechanism by which electric field facilitates DNA transport across these barriers is still speculative and poorly characterized, although studies have suggested diffusion, electro-osmosis, and electrophoresis as potential driving forces (Michel, Elgizoli et al. 1988; Dimitrov and Sowers 1990). Of these three possibilities, electrophoresis has been the subject of the most investigation although results are still contradictory. The works of Kleinchen et al. and Bureau et al. provide supporting evidence that electrophoresis has a substantial effect on DNA delivery across the cell membrane and consequently, on transfection efficiency. Kleinchen et al. utilized a cell monolayer cultured on a porous

film to observe a 10-fold increase in transfection efficiency when pulses of a polarity which induced DNA electrophoresis towards the monolayer were applied versus pulses of inverse polarity (Kleinchin 1991). Bureau et al. corroborated these findings by showing significantly greater transfection efficiency in vivo when a series of pulses consisting of one short, high-voltage 'electroporating' pulse followed by four long, low-voltage electrophoresis-inducing pulses was used compared to the single high-voltage pulse or the four low-voltage pulses alone (Bureau, Gehl et al. 2000). However, contradictory findings were determined by Liu et al., which showed no difference in gene expression in vivo between electric pulses of alternating polarity versus pulses of consistent polarity. If electrophoresis is a significant mechanism of DNA transmembrane transport, the latter pulse type should yield higher expression levels. They also showed no impact on transfection efficiency when the electrophoretic effect was diminished by increasing the viscosity of the pulsing buffer with 10% Ficoll or increasing the concentration of Mg^{2+} cation to increase shielding of the polyanionic DNA (Liu, Heston et al. 2006).

Alternatively, electrically-induced endocytosis of macromolecules has been witnessed to be a side effect of pulsed, electric field. Antov et al. observed enhanced membrane absorption of bovine serum albumin and dextran due to non-permeabilizing low electric field pulses, which was followed by increased uptake of these macromolecules (Antov, Barbul et al. 2005). β -galactosidase added well after electric

field pulsing was seen to localize within large vesicles and macropinocytosis was implicated when post-pulse uptake of the enzyme diminished when cells were treated with the actin-depolymerizing drug, colchicine (Rols, Femenia et al. 1995). Human fibroblasts showed increased uptake of fluorescent BSA-labeled membrane moieties for up to 90 minutes after electric field treatment (Glogauer, Lee et al. 1993). All of these studies suggest increased endocytosis of non-DNA macromolecules to be an aftereffect of pulsed, electric field but does not directly implicate endocytosis as being the mode of DNA internalization during electric field pulsing.

The studies highlighted in Chapter 3 provide seminal evidence directly implicating endocytosis in electrically-induced DNA uptake. The same combination approach of using pharmacological inhibition and RNA interference will be adopted here once again to identify and compare the specific endocytic pathways induced by electric field to facilitate DNA transmembrane transport in two different cell lines.

4.2 Materials & Methods

4.2.1 Cell Culture

Normal, adult human dermal fibroblasts (NHDF) (Lonza, Basel, Switzerland) were cultured in T75 flasks in high glucose Dulbecco's modified Eagle's medium (Gibco 11960) (Invitrogen, Carlsbad, CA) supplemented with 20% fetal bovine serum (Sigma,

St. Louis, MO), 25 µg/mL gentamicin (Gibco), 1X GlutaMAX, 1X MEM non-essential amino acids, 1X sodium pyruvate, and 1X β-mercaptoethanol (Invitrogen). HT29, human colon adenocarcinoma, cells (ATCC, Manassas, VA) were cultured in T75 flasks in high glucose Dulbecco's modified Eagle's medium (Gibco 11995) (Invitrogen) supplemented with 10% bovine growth serum (Hyclone, Logan, UT) and penicillin/streptomycin (Gibco 15140) (Invitrogen). The cells were incubated at 37°C in 5% CO₂ and 95% air and passaged every 2-3 days for HT29 and every 4-5 days for NHDFs. NHDFs were used between passages 4 to 11.

In preparation for electrotransfection (see Section 4.2.3), 50-70% confluent HT29 cells and 90% confluent NHDFs were treated with 0.25% trypsin-EDTA (Invitrogen) for 10-15 min at 37°C, washed with serum-containing medium to neutralize trypsin activity, and harvested by centrifugation. Cells were resuspended in the electroporation buffer OptiMEM I Reduced Serum Media (Invitrogen) and cell density was determined using a hemacytometer.

4.2.2 Plasmid

A 4.7 kbp plasmid (pEGFP-N1, Clontech, Palo Alto, CA), encoding enhanced green fluorescent protein (GFP), was amplified by transformed, Z-competent (Zymo Research, Orange, CA) DH5α and Top10 *E. coli* strains and purified using the Qiagen Plasmid Giga Prep Kit (Qiagen, Valencia, CA), as per manufacturers' protocols.

4.2.3 Electrotransfection

For both NHDF and HT29 cells, 1 million cells were suspended in OptiMEM I as the electroporation buffer and mixed with 6 μg pEGFP-N1 to achieve a final sample volume of 100 μL . Samples were incubated on ice for 10 min (with occasional flicking to resuspend cells) before being transferred into BTX disposable 4-mm gap aluminum cuvettes (Harvard Apparatus, Holliston, MA). Cells were then subjected to electric field pulse treatments using a BTX ECM 830 Square Wave Electroporation System (Harvard Apparatus). NHDFs were subjected to 8 pulses at 400 V/cm, 5 msec duration, and 1 Hz frequency and HT29 cells were subjected to 6 pulses at 600V/cm, 5 msec duration, and 1 Hz frequency. Electric pulse protocols had been optimized for each line to achieve optimal transfection efficiency and cell viability. Samples were left undisrupted in the cuvette for 10 min at room temperature post electrotransfection, to promote cell recovery and resealing of pores in the membrane. Samples were then seeded in fresh media in 6-well plates and GFP expression was quantified using flow cytometry following 24 hrs of incubation.

4.2.4 Treatment of Cells with Pharmacological Inhibitors of Endocytosis

Stock solutions of the endocytic inhibiting drugs, chlorpromazine hydrochloride, genistein, and amiloride hydrochloride hydrate (Sigma Aldrich, St. Louis, MO) were

prepared in DMSO at concentrations of 5 mg/ml, 25 mg/ml, and 130 mg/ml, respectively, and stored at -20°C. NHDF and HT29 cells were seeded in 6-well plates to achieve 80-90% confluency within 24 hours and 50-60% confluency within 48 hours, respectively. Media was aspirated and adherent cells were washed twice with PBS without Ca²⁺ and Mg²⁺. 2 mL of OptiMEM was added to each well and appropriate volumes of each drug stock were added to achieve final drug concentrations of 50 µM chlorpromazine, 300 µM genistein, and 300 µM amiloride for HT29 cells (Papatheodorou, Zamboglou et al.) (Saovapakhiran, D'Emanuele et al. 2009) (Bermudez and Young 1994; Wells, Jechorek et al. 1999; Nemeth, Deitch et al. 2002; Stuart, Eustace et al. 2002; Kojic, Wiseman et al. 2008) and 28 µM chlorpromazine, 200 µM genistein, and 2.5 mM amiloride for NHDFs (Hsu and Mitragotri ; Wiranowska, Colina et al. ; Zhang, Hu et al. ; Wang, Rothberg et al. 1993; Puri, Watanabe et al. 2001; Bardor, Nguyen et al. 2005). For the control groups, equivalent volumes of DMSO without drugs were added. Cells were incubated at 37°C in 5% CO₂ and 95% air for 1 hr and subsequently washed with PBS without Ca²⁺ and Mg²⁺. Cells were trypsinized, washed again with serum-containing media, and re-suspended in OptiMEM at a density of 1x10⁷ cell/mL. They were subsequently transfected with GFP-encoding plasmid using the aforementioned electrotransfection protocol (See Section 4.2.3) to investigate the effects of the various drug treatments on electrotransfection efficiency.

4.2.5 Flow Cytometry

DMEM was aspirated from each well and adherent cells were washed twice with PBS without Ca^{2+} and Mg^{2+} . The cells were then detached by trypsinization, washed with serum-rich DMEM to neutralize trypsin activity, and resuspended in 350-400 μL of 5 $\mu\text{g}/\text{mL}$ propidium iodide (PI) in PBS. The BD FACScan flow cytometer (Becton Dickinson, Franklin Lakes, NJ), equipped with an argon laser with excitation wavelength of 488 nm and three fluorescent detectors (530/30, 585/42, 670LP), was used for simultaneous dual detection of GFP and PI fluorescence. Forward and side light scatterings were used as independent variables to exclude debris and isolate the cell population of interest. Compensation was set between 20-25% to resolve spectral emission overlap between the two channels and 10,000 events were collected for each sample. Autofluorescence was corrected for each experimental group by using control sample groups treated with the same experimental conditions and subjected to the same electric pulse protocols but without GFP-encoding pDNA. BD CELLQUEST™ Software was used for data acquisition and analysis. Electrotransfection efficiency was expressed as the percentage of total viable cells that expressed GFP (PI negative, GFP positive).

4.2.6 Small, interfering RNA (siRNA) Transfection

NHDFs and HT29 cells were transfected with Stealth small interfering RNA (siRNA) oligos (Invitrogen) directed against clathrin heavy chain (CHC), caveolin-1

(CAV1), and Rab34 or the Stealth RNAi negative control duplex of similar GC content (Invitrogen) using the Amaxa Nucleofector II System (Amaxa, Cologne, Germany). For each protein target, two siRNA oligos targeting different specific sequences within its gene were used. The targeted sequences and their relative GC contents, which is important for pairing them with the appropriate Stealth RNAi control duplex, are as follows:

CHC, siRNA-1 (Low GC): 5'-CCGGAAATTTGATGTCAATACTTCA-3'

CHC, siRNA-2 (Low GC): 5'-GAGTGCTTTGGAGCTTGTCTGTTTA-3'

CAV1, siRNA-1 (Med GC): 5'-CCCACCTCTTTGAAGCTGTTGGGAAA-3'

CAV1, siRNA-2 (Low GC): 5'-TCCGCATCAACTTGCAGAAAGAAAU-3'

RAB34, siRNA-1 (Low GC): 5'-AATTCTCGGACATTCTCACCAGTGA-3'

RAB34, siRNA-2 (Med GC): 5'-AATCGTTCCATCTCGAAGTCCACTC-3'

siRNA transfections were carried out using the Human Dermal Fibroblast (NHDF-Adult) Nucleofector Kit (Amaxa) and program U-023 on the Nucleofector II System for NHDFs and Nucleofector Kit R and program W-017 for HT29, according to manufacturer's protocols. HT29 were grown to 60-70% confluency and NHDFs to 90% confluency for siRNA transfection. For transfection of HT29 with siRNA sequences directed against all three proteins, 2×10^6 cells were transfected with 300 nM of siRNA or

negative control duplex in a sample volume of 100 μL , seeded in 6 well plates, and incubated for 48 hours. For transfection of NHDFs with the siRNA sequences directed against CAV1 and RAB34, 5×10^5 cells were transfected with 300 nM siRNA or negative control duplex in a sample volume of 100 μL , seeded in 6 well plates, and incubated for 48 hours. After the incubation period, cells were harvested for electrotransfection experiment or Western Blot analysis.

For transfection of NHDFs with siRNA sequences directed against CHC, two rounds of siRNA transfection using two different transfection methods were required to achieve sufficient knockdown of the target protein. On day 1, 5×10^5 NHDF cells were transfected with 1.2 μM siRNA or negative control duplex using the Amaxa Nucleofector II System and seeded in 6 well plates. After 48 hours of incubation, cells reached 50-70% confluency and were transfected again on day 3 with siRNA using Lipofectamine RNAiMax transfection reagent (Invitrogen), according to the manufacturer's forward transfection protocol. In short, cells were treated with 50 nM (final concentration) of siRNA mixed with 7.5 μL RNAiMax per well and incubated overnight. On day 4, cells were split 1:2 to achieve <90% confluency by the next day. On day 5, cells were harvested either for electrotransfection experiment or Western Blot analysis.

4.2.7 Western Blot Analysis

Cells were subjected to the aforementioned siRNA transfection treatments in preparation for immunoblot analysis. Cells were harvested by trypsinization after the appropriate post-siRNA incubation periods to determine protein expression levels at the times of electrotransfection treatment. Total protein content was isolated using a 10:1 mixture of CellLytic M Cell Lysis Reagent (Sigma Aldrich) to Protease inhibitor cocktail (Sigma Aldrich) and quantified using Pierce BCA Protein Assay Kit (Thermo Scientific, Rockford, IL). 7-30 μg (depending on the cell line and target protein being probed) of total protein extract per well was separated in a 12% Ready Gel Tris-HCl polyacrylamide gel (Bio-Rad, Hercules, CA), transferred onto PVDF membrane (Bio-Rad), blocked for 2-3 hours at room temperature in 5% milk, 20 mM Tris, 500 mM NaCl, 0.1% Tween20 (pH 7.5) and incubated overnight at 4°C with primary antibodies: rabbit polyclonal anti-caveolin-1 (Santa Cruz Biotech, Santa Cruz, CA), rabbit polyclonal anti-Rab34 (Abcam, Cambridge, MA), rabbit polyclonal anti-clathrin heavy chain (Abcam) and rabbit polyclonal anti-actin (Santa Cruz) as a loading control. Membrane was then probed with goat anti-rabbit secondary antibody conjugated to horseradish peroxidase (Santa Cruz) for 35 min at room temperature, developed with SuperSignal West Pico Chemiluminescent Substrate (Thermo Scientific), and visualized with Amersham Hyperfilm™ ECL film (GE Healthcare, Buckinghamshire, UK).

4.2.8 Statistical Analysis

Difference between experimental groups was compared using the nonparametric Mann-Whitney U test. A difference was considered to be significant if the P value was < 0.05.

4.3 Results

4.3.1 Effect of endocytic inhibitors on electrotransfection efficiency.

Three different pharmacological inhibitors, chlorpromazine, genistein, and amiloride, were used to transiently inhibit clathrin-mediated endocytosis, caveolae-dependent endocytosis, and macropinocytosis, respectively, in NHDF and HT29 cells.

Chlorpromazine (CPZ) specifically inhibits clathrin-mediated endocytosis by anchoring clathrin and the adaptor protein 2 (AP2) complex to intracellular endosomes and preventing coated pit assembly along the cell membrane (Wang, Rothberg et al. 1993).

Genistein is a tyrosine kinase inhibitor that inhibits caveolae-dependent endocytosis by preventing actin depolymerization of the local cortical actin cytoskeleton, which must precede internalization of caveolar vesicles, and by also preventing recruitment of dynamin II to facilitate vesicle scission (Pelkmans, Puntener et al. 2002). The mechanism by which amiloride inhibits macropinocytosis is still uncertain but it has been shown that local acidification occurs in the submembranous region at site of

macropinocytosis, which is eradicated by Na^+/H^+ exchange. Amiloride is a known inhibitor of Na^+/H^+ exchangers, thereby causing the build up of acidity at these macropinocytic sites. Furthermore, it was found that GTPases involved in actin remodeling was highly sensitive to submembranous pH. Hence, amiloride may potentially inhibit macropinocytosis by lowering the pH at these sites, leading to impaired actin polymerization, which is crucial for macropinocytosis (Koivusalo, Welch et al. 2010). Treatment concentrations of each drug for each cell line were determined from literature review (see Section 4.2.4 of Methods & Materials).

HT29 cells treated with 50 μM chlorpromazine (CPZ) for 1 hour prior to electrotransfection with a GFP-encoding plasmid, exhibited a ~40% reduction ($P < 0.05$) in electrotransfection efficiency (eTE) compared to a control group treated with an equivalent volume of DMSO vehicle (**Figure 4.1A**). When treated with 300 μM genistein or 300 μM amiloride targeting caveolae-dependent endocytosis and macropinocytosis, respectively, HT29 cells showed no diminishment in eTE. NHDFs, on the other hand, showed no response in eTE when treated with 28 μM CPZ and 200 μM genistein, but exhibited a 70% decrease ($P < 0.05$) in eTE when treated with 2.5 mM amiloride prior to electrotransfection (**Figure 4.1B**).

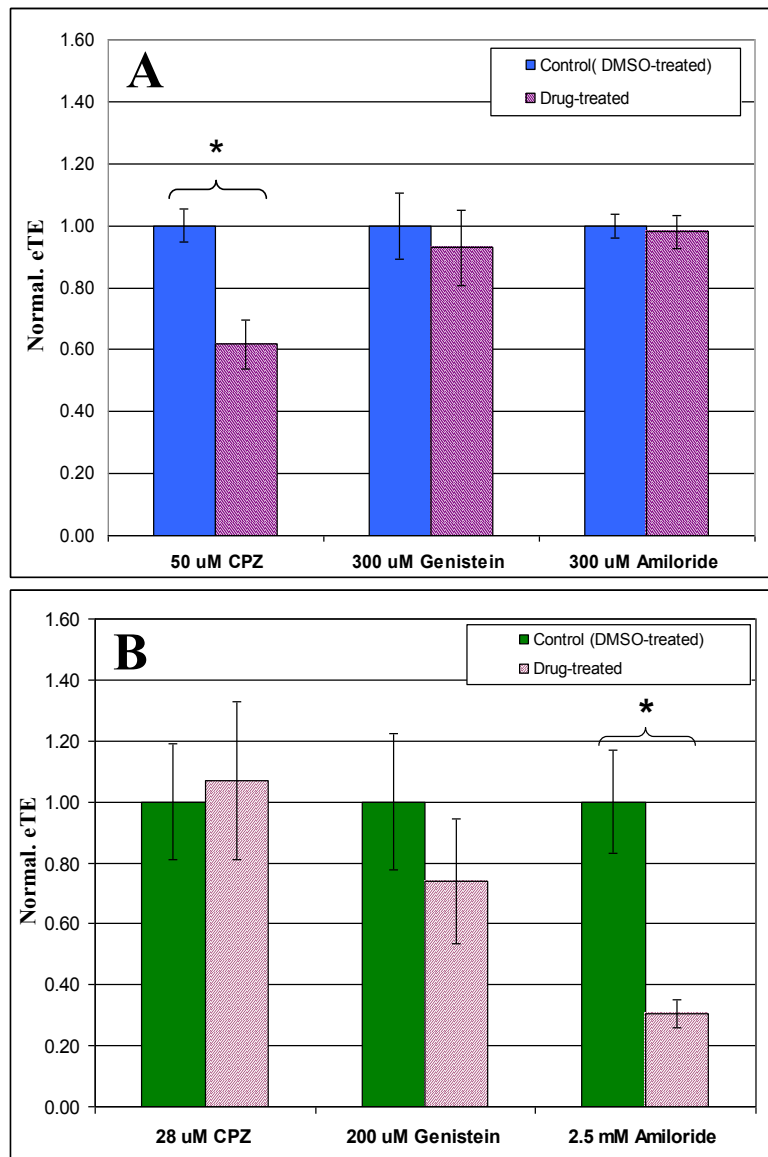


Figure 4.1: Effect of endocytic inhibitor treatment on electrotransfection efficiency (eTE). (A) HT29 cells were treated with 50 μ M chlorpromazine (CPZ), 300 μ M genistein, and 300 μ M amiloride, and (B) NHDFs were treated with 28 μ M CPZ, 200 μ M genistein, and 2.5 mM amiloride, or their equivalent volumes in drug vehicle DMSO (Control) for 1 hr prior to electrotransfection with GFP-encoding pDNA. Flow cytometry was used to quantify eTE after cells were cultured at 37°C for 24 hrs post-transfection. eTE, defined as the percent of live cells expressing GFP, for each drug treated group was normalized by their respective control. N = 4–7 independent trials. * P < 0.05 (Mann-Whitney U test).

4.3.2 Effect of siRNA knockdown on electrotransfection efficiency

To target clathrin-mediated endocytosis, caveolae-dependent endocytosis, and macropinocytosis, clathrin heavy chain (CHC), caveolin-1, and Rab34 were chosen as the target proteins for siRNA-directed expression knockdown, respectively. For each protein, NHDFs and HT29 cells were transfected via an Amaxa Nucleofector II System with two specific, small interfering RNA (siRNA-1 and siRNA-2) directed against two different nucleotide sequences within the encoding gene or negative control, nonspecific siRNA duplexes of comparable GC content.

For all three target proteins, HT29 cells were transfected with 300 nM siRNA and total protein extract were harvested from cells after a 48h post-siRNA-transfection period. Western blot (**Figure 4.2**) shows almost complete abolishment of the caveolin-1 protein for both CAV1, siRNA-1 and CAV1, siRNA-2 treated groups, when compared to their corresponding controls of comparable GC content. Both CHC, siRNA-1 and CHC, siRNA-2 treated HT29 cells exhibited reduced, albeit not entirely eliminated, protein expression levels of clathrin heavy chain compared to the control case. For detection of Rab34 protein (~29 kDa), 10 µg of total protein were initially loaded into each well and failed to produce Rab34 bands in any of the lanes, including the control groups treated with non-specific, siRNA duplexes (results not shown). Hence, total protein content was increased to 30 µg per well (shown in **Figure 4.2**) yet still produced no detectable Rab34 bands in any of the control or sample groups. Due to the high protein mass per well and

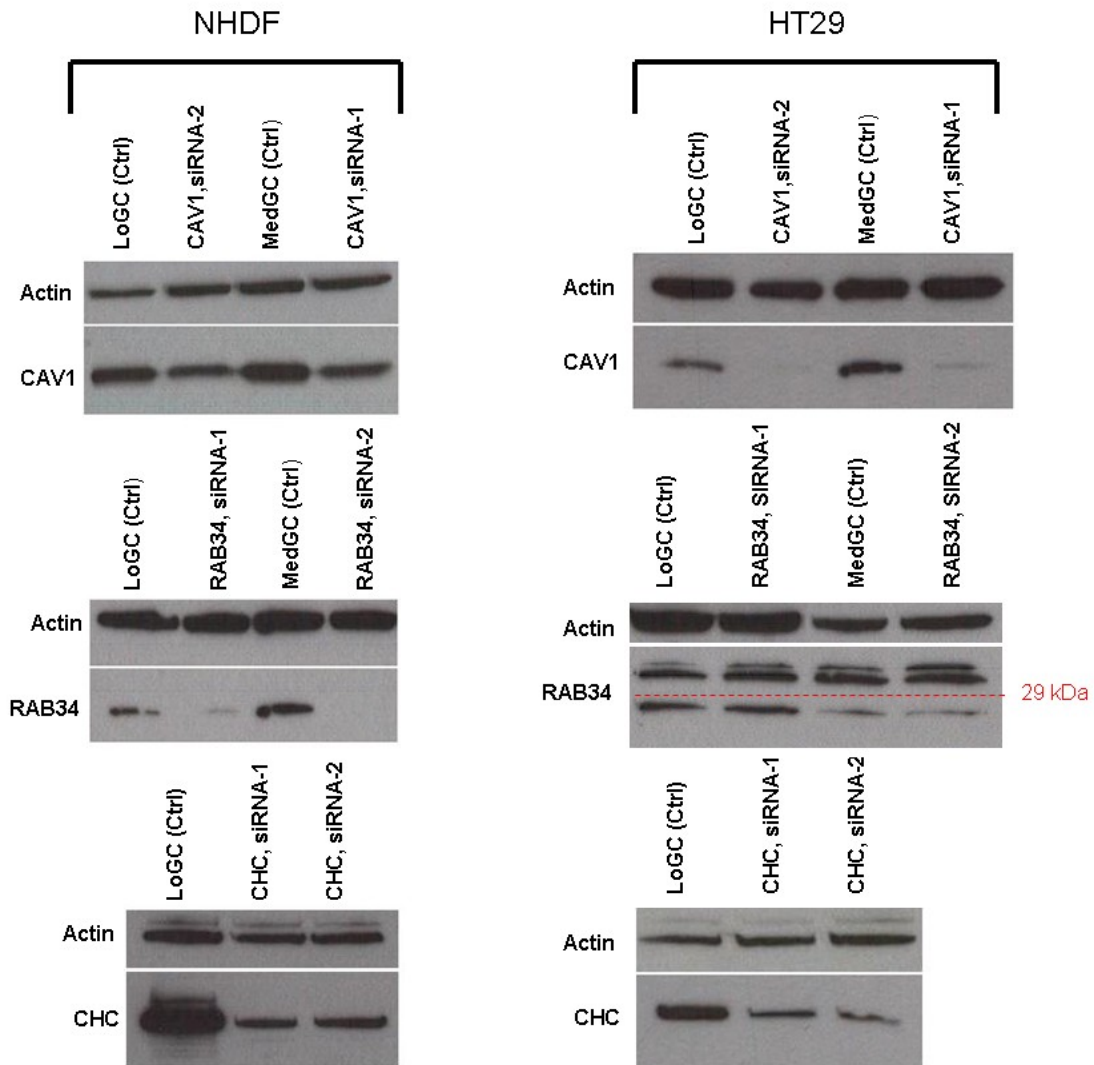


Figure 4.2: Western blot of target protein knockdown. For each target protein, NHDF and HT29 cells were transfected with two specific siRNA oligos directed against two different sequences (i.e., siRNA-1 and siRNA-2) and control siRNA duplexes of comparable GC content. HT29 exhibited no band for Rab34 (most likely due to low endogenous expression levels) although non-specific bands were detected above and below the band of interest. Actin was used as the loading control. Representative images shown of two independent experiments.

high antibody concentration used to probe for Rab34, nonspecific bands of greater and lower molecular weight appeared above and below, respectively, where our protein

band of interest should have been detected. It is speculated that the absence of Rab34 band across all groups is attributed to low endogenous levels of the protein in HT29.

For knockdown of CAV1 and Rab34 in NHDFs, cells were transfected with 300 nM siRNA and protein extracts were harvested after a 48 hour post-siRNA transfection incubation period. Western blot shows diminished Cav1 protein expression levels for both the CAV1, siRNA-1 and CAV1, siRNA-2 treated groups and almost complete protein knockdown of Rab34 for both RAB34, siRNA-1 and RAB34, siRNA-2 treated groups. 300 nM siRNA was insufficient in achieving protein expression reduction of clathrin heavy chain in NHDFs after 48 hours (not shown). This was speculated to be attributed to a potentially prolonged half-life of the clathrin heavy chain (CHC) in NHDF, resulting in sustained high intracellular concentration of CHC even after 48h, despite diminished mRNA levels and inhibited protein production. To overcome this issue, NHDFs were subjected to two rounds of siRNA transfection spaced over 5 days to permit sufficient time for degradation of existing CHC levels while maintaining low intracellular mRNA levels and inhibiting the generation of new CHC proteins. NHDFs were transfected with 1.2 μ M siRNA directed against CHC via the Amaxa Nucleofector II System on day 1, transfected again with 50 nM siRNA via Lipofectamine RNAiMax on day 3, and harvested for protein extract on day 5. **Figure 4.2** shows this siRNA treatment protocol to be sufficient in diminishing protein expression of CHC for both the CHC, siRNA-1 and CHC, siRNA-2 treated groups, when compared to the control.

Having confirmed protein expression knockdown via western blot analysis, NHDFs and HT29 cells were then subjected to the same siRNA transfection protocols followed by electrotransfection with a GFP-encoding plasmid. Transfection efficiency was quantified as percentage GFP expression after 24 hours and shown in **Figures 4.3** and **Figure 4.4** for HT29 cells and NHDFs, respectively. For HT29, the CHC, siRNA-2 treated group exhibited a significant change in eTE from ~50% for the control to ~36% for the treated case ($P < 0.05$) whereas all other siRNA-treated group exhibited no change in eTE compared to their corresponding controls. For NHDFs, eTE exhibited significant reductions from 12% for the control case to 9% for the CAV1, siRNA-2 treated case and to 8% for the Rab34, siRNA-1 treated case.

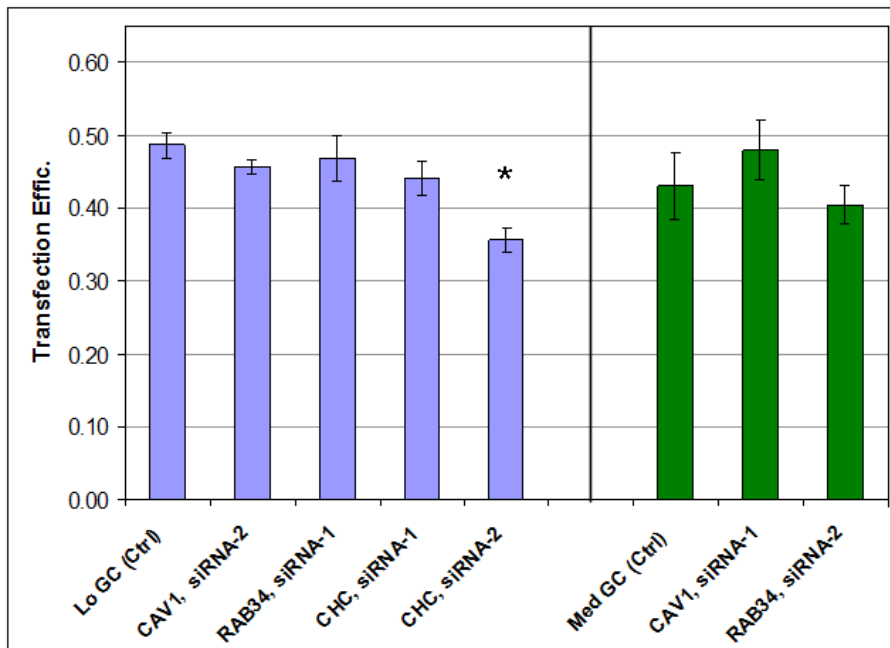


Figure 4.3: Effect of siRNA knockdown of caveolin-1 (CAV1), Rab34, and clathrin heavy chain (CHC) on electrotransfection efficiency of HT29. For each targeted protein, HT29 cells were transfected with either of two siRNA oligos (siRNA-1 and siRNA-2) directed against two different nucleotide sequences or the corresponding control siRNA. After siRNA transfection, cells were incubated for 48 hours and subjected to pDNA electrotransfection. siRNA oligos were grouped with the control siRNA of similar GC content in the chart above. Error bars denote standard error of N=4-5 independent trials. * denotes a statistically significant difference between the treated group and its control. $P < 0.05$ (Mann-Whitney U test).

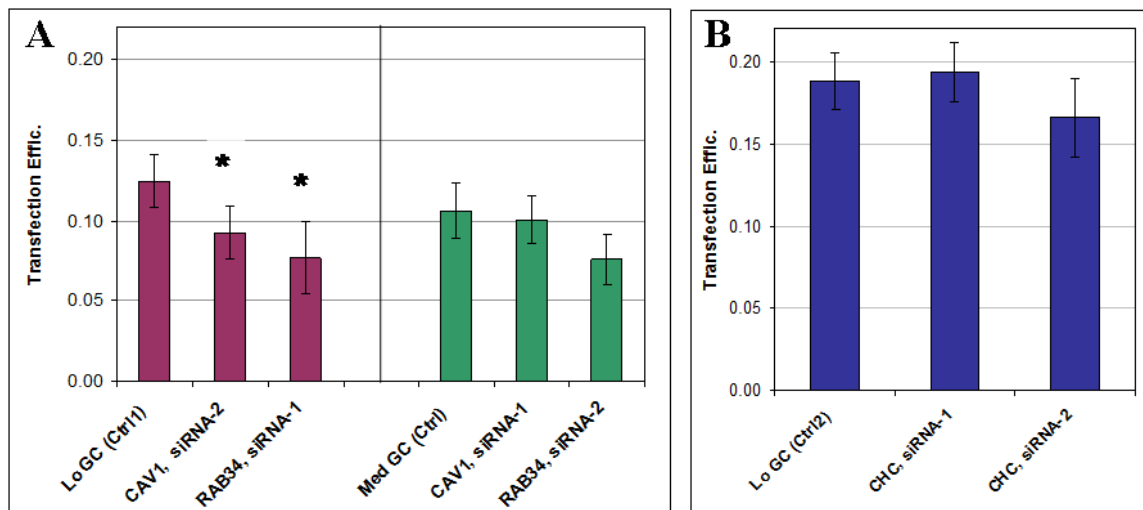


Figure 4.4: Effect of siRNA knockdown of caveolin-1 (CAV1), Rab34, and clathrin heavy chain (CHC) on electrotransfection efficiency on NHDF. For each targeted protein, NHDF cells were transfected with either of two siRNA oligos (siRNA-1 and siRNA-2) directed against two different nucleotide sequences or the corresponding control siRNA. (A) For knockdown of CAV1 and Rab34, cells were transfected with 300 nM siRNA or control duplex using the Amaxa Nucleofector II and incubate 48 h before pDNA electrotransfection (B) For knockdown of CHC, cells were transfected with 1.2 μ M siRNA or control duplex using the Amaxa Nucleofector on day 1, transfected again with 50 nM siRNA using Lipofectamine RNAiMax on day 3, and subjected to pDNA electrotransfection on day 5. siRNA oligos were grouped with the control siRNA of similar GC content in the charts above. Error bars denote standard error of 6-9 independent trials. * denotes a statistically significant difference between the treated group and its control. $P < 0.05$ (Mann-Whitney U test). LoGC(Ctrl1) and LoGC(Ctrl2) denotes control groups transfected with the Stealth control duplex of Low GC content, using the transfection protocols described in (A) and (B), respectively.

4.4 Discussion

4.4.1 Pharmacological inhibition of electrotransfected pDNA delivery

The use of pharmacological inhibitors has been an established approach for studying the endocytic pathways involved in the internalization of ligands, markers, and non-viral gene carriers, such as cationic liposomes and polymers (Rejman, Bragonzi et al. 2005; Rejman, Conese et al. 2006; Vercauteren, Vandenbroucke et al. 2009). A

variety of chemical inhibitors of endocytosis have been developed and screened to selectively target different endocytic pathways, especially the three best-characterized mechanisms of clathrin-mediated endocytosis, caveolae-dependent endocytosis, and macropinocytosis. Elucidating the internalization means and intracellular trafficking routes of genes and gene carriers provides insightful information regarding the efficiency of different endocytic pathways in leading to ultimate gene expression, which can be utilized to design and/or modify properties of the gene/gene carrier to either target certain pathways or circumvent certain endocytic obstacles/barriers.

We have thus adopted this strategy to study the internalization of naked plasmid DNA when electroporation/electrotransfection is used as the gene delivery method. Chlorpromazine (CPZ), genistein, and amiloride are established specific inhibitors of clathrin-mediated endocytosis, caveolae-dependent endocytosis, and macropinocytosis, respectively, and their inhibitory working concentrations for the NHDF and HT29 cell lines were obtained from an extensive literature review (See Section 4.2.4 of Methods & Materials). It is important to note that in this study, NHDFs and HT29 cells are treated with different concentration of each drug. This is not unusual as it has been demonstrated that different empirically determined, working concentrations of each drug are required to exert their inhibitory effect on their target pathway in different cell lines (Vercauteren, Vandenbroucke et al. 2009).

The two cell lines tested, NHDFs and HT29, showed different responses to the endocytic inhibitors. Whereas HT29 cells exhibited a significant 40% decrease in eTE only when cells were pretreated with 50 μ M CPZ prior to electrotransfection, NHDFs showed no change with CPZ or genistein treatment but a dramatic reduction in eTE of 70% when treated with amiloride (**Figure 4.1**). This implicates clathrin-mediated endocytosis as the dominant mode of pDNA internalization in HT29 and macropinocytosis as the preferred path of pDNA uptake in NHDFs, when subjected to electrotransfection. Although endocytic drug treatment did yield significant ($P < 0.05$) and substantial diminishments in eTE for both HT29 and NHDF, gene expression was not completely abolished for either cell lines. This result may be caused by several possibilities. The various drug treatments, although effective in reducing transport along their targeted endocytic pathways, may not completely inhibit their activities. Thus, some residual degree of pDNA uptake via clathrin-mediated endocytosis and macropinocytosis may still exist in CPZ-treated HT29 and amiloride-treated NHDFs, respectively, to account for the remaining transfection efficiency. Another likely possibility for this result exists in a limitation of the experimental protocol. After the one hour drug treatment, cells were washed with PBS, subjected to trypsinization for 5-10 min, resuspended in serum-containing media, counted via a hemacytometer, spun down, resuspended in OptiMEM with pDNA at the appropriate cell density (see Section 4.2.4), and incubated on ice for 10 minutes prior to finally receiving electrotransfection

treatment. This amounts to approximately a 20-25 minutes delay after drug exposure before cells are electrotransfected with pDNA. This time lag could be significant enough to allow for some drug clearance from the cells and partial recovery of the targeted endocytic pathways. This translates again to impaired, but not completely inhibited, endocytosis by the time electrotransfection of cells takes place. Lastly, alternative endocytic pathways, not targeted by the endocytic inhibitors used in this study, may exist in both cell lines to account for the residual transfection efficiency. As briefly outlined in the introduction, there exists poorly characterized clathrin- and caveolae-independent, non-macropinocytic pathways, for which endocytic drugs have not been developed. Although poorly understood, these endocytic pathways still play a crucial role in many cellular functions and may contribute to the uptake, intracellular trafficking, and ultimate gene expression of electrotransfected pDNA.

Pharmacological inhibition provides a fast, easy to use strategy to induce transient impairment of targeted endocytic pathways. While it offers many advantages, it also suffers from certain limitations, the main issue being the potential for poor specificity and variable efficacy. Poor specificity could arise from unintended effects on alternate endocytic mechanisms other than the targeted pathway, as well as disruption of other cellular processes, molecules, and activity that have an indirect effect on endocytosis. An example of the latter case is the disruption of the actin cytoskeleton, involved in formation and invagination of vesicles in several endocytic pathways, as

well as in the organization and function of various cell membrane proteins and components. Indirect drug effects on this highly regulated cellular process would likely lead to aberrant endocytic behavior (Ivanov 2008). Efficacy of pharmacological inhibitors has also been shown to vary in a cell-dependent manner, even with optimization for each particular cell line (Vercauteren, Vandenbroucke et al. 2009).

Chlorpromazine (CPZ), used in our study to target clathrin-mediated endocytosis, has been shown to block phagocytosis in neutrophils and macrophages (Elferink 1979) (Watanabe, Hirose et al. 1988) and potentially also macropinocytosis (Ivanov 2008). These effects on alternate pathways may result from the fact that it is an amphipathic molecule that embeds readily into the phospholipid bilayer to alter membrane fluidity and consequently, membrane invagination behavior. These side effects may also stem from the drug's purported inhibitory effect on phospholipase C, a regulatory molecule of actin polymerization and macropinocytosis (Ogiso, Iwaki et al. 1981; Wells, Ware et al. 1999; Amyere, Payraastre et al. 2000; Ivanov 2008). A systematic study of the efficacy and specificity of various endocytic inhibitors in several cell lines showed CPZ to inhibit uptake of human transferrin, a specific marker of clathrin-mediated endocytosis, in a cell line specific manner, with some cell lines exhibiting no effect to treatment. The same study also investigated genistein, used in our study to target caveolae-dependent endocytosis, in inhibiting the uptake of LacCer, a specific marker for lipid raft dependent endocytosis. While genistein exhibited high efficacy in

reducing LacCer uptake across all cell lines, it also caused a dramatic 80% diminishment in the clathrin-mediated uptake of transferrin in one particular cell line (Vercauteren, Vandenbroucke et al. 2009). This effect is not surprising considering that genistein, although a commonly used inhibitor of caveolae-mediated endocytosis (Sieczkarski and Whittaker 2002; Gabrielson and Pack 2009; Rea, Gibly et al. 2009), is a nonspecific tyrosine kinase inhibitor that may have additional effects on molecules involved in or shared with other endocytic pathways.

Amiloride, used in our study to target macropinocytosis, has also illustrated alternate inhibitory effects on clathrin-mediated uptake of junctional protein complexes in epithelial cells (Ivanov, Nusrat et al. 2004) and of receptor-bound albumin in opossum kidney cells (Gekle, Freudinger et al. 2001). An amiloride analogue was also shown to cause disruption of actin cytoskeleton dynamics in fibroblasts leading to inhibited cell motility, pseudopodial retraction, and detachment from substrate (Lagana, Vadnais et al. 2000). This drug-induced disassembly of actin fibers would logically also affect multiple actin-dependent endocytic pathways.

4.4.2 Effect of siRNA silencing of endocytic proteins on electrotransfection efficiency

Given the specificity and efficacy issues encountered with using pharmacological drugs to study endocytosis, it is necessary to corroborate these findings using another strategy. Molecular biological methods such as siRNA silencing provide the advantages

of high specificity, superior efficacy, minimal toxicity, and sustained inhibition of the target protein or mechanism. This strategy was employed to impair the same three endocytic pathways by targeting crucial proteins exclusively implicated for each pathway. For inhibition of clathrin-mediated endocytosis, siRNA silencing was directed against the clathrin heavy chain, an important component of the clathrin coat protein that dictates its triskelion structure and permits its assembly into polygonal lattices at clathrin-coated pits (CCP) along the membrane (Conner and Schmid 2003). For inhibition of caveolae-dependent endocytosis, siRNA silencing was directed against caveolin-1, the main coat protein found within caveolae in most cells that is responsible for the formation and structural stability of caveolae. Macropinocytosis was inhibited with siRNA directed against Rab34, a member of the Rab family of small GTPases that has been found to localize in regions of membrane ruffling, the predominant site for macropinocytosis, and deemed necessary in the formation of macropinosomes (Sun, Yamamoto et al. 2003).

Western blot analysis was used to verify reduced protein expression levels after siRNA transfection. siRNA-treated cells were then electrotransfected with GFP-encoding plasmid and transfection efficiency was measured the following day to determine the effect of endocytic knockdown on pDNA internalization. It is important to note from **Figure 4.2** that for some cases, one or both siRNA-treated groups for each target protein result in diminished, but not completely abolished, levels of protein

expression. This incomplete gene silencing of the target protein has been commonly witnessed throughout literature (Elbashir, Harborth et al. 2001; Holen, Amarzguioui et al. 2002; Ji, Wernli et al. 2003) as a result of using a single chemically synthesized siRNA. Ji et al. determined that single siRNA sequences downregulate target mRNA and protein expression in a dose-dependent manner up to a certain plateau threshold (ranging from 20%-70% depending on the target protein and siRNA sequence), beyond which increasing siRNA concentration yields no additional inhibitory effect. They speculate the possible causes for this behavior to be the efficiency of the siRNA transfection and/or the half-life of the target protein. Cotransfecting cells with two or more different siRNA duplexes was shown to be an effective strategy in overcoming this barrier and enhancing gene silencing (Ji, Wernli et al. 2003). An important observation to note from their study is that even in their best case scenario, where a combination of 3 siRNA duplexes were used to target a protein, the expression level diminished by 90% but was still not completely abolished. Secondly, it was also shown that a certain siRNA-induced reduction in target mRNA and protein expression levels does not always result in a comparable reduction in the functional effect of that protein. Specifically, HEK293 cells were transfected with 20 nM of either of two siRNA duplexes targeting the apoptosis-inducing Fas-ligand (FasL), which resulted in a 20% and 30% decrease in FasL protein expression but yielded only 10% and 20% inhibition of FasL-mediated apoptosis, respectively. This second observation is mirrored in our study,

whereby qualitatively substantial reductions in protein expression (**Figure 4.2**) produced only modest yet statistically significant effects on transfection efficiency (**Figure 4.3** and **4.4**).

For HT29 cells, only one group treated with one of the two siRNA sequences directed against clathrin heavy chain exhibited a significant reduction ($P < 0.05$) in eTE from 49% for the control (Low GC) case to 36% for the treated group (**Figure 4.3**). NHDFs, on the other hand, showed diminished eTE with both caveolin-1 (9%) and Rab34 (8%) expression knockdown when compared to the control case (12%) (**Figure 4.4**). The endocytic pathways implicated in electric field-mediated pDNA uptake for each cell line using siRNA silencing agree with the findings determined using the pharmacological approach. Chlorpromazine treatment and CHC knockdown, targeting clathrin-mediated endocytosis, in HT29 both resulted in reduced eTE whereas amiloride and Rab34 knockdown, targeting macropinocytosis, led to eTE reductions in NHDFs. Interestingly, siRNA knockdown of caveolin-1 (CAV1) in NHDFs resulted in a 25% decrease in eTE from 12% (control) to 8% (treated), which also implicates caveolae-mediated endocytosis as an additional mechanism of electric field-mediated pDNA internalization in NHDFs. This finding could not be conclusively supported by the pharmacological results, which showed a substantial, although statistically insignificant ($P=0.20$) reduction in eTE of ~30% when NHDFs were treated with genistein.

An interesting point to note is the modest reductions in eTE in both cell lines resulting from siRNA treatment in comparison to using pharmacological inhibitors. CHC knockdown in HT29 yielded a ~ 27% eTE decrease compared to the control case whereas CPZ drug treatment induced a 40% drop. The difference is more dramatic in NHDFs, in which siRNA-directed knockdown of Rab34 produced a 33% reduction in eTE but amiloride caused a 70% diminishment. The disparity between the two different methods is most likely attributed to the duration of their induced inhibitory effects. siRNA knockdown causes a gradual and sustained reduction in protein expression levels whereas the effect of pharmacological agents are immediate and short-lived. Endocytosis being a crucial process necessary for cellular homeostasis and viability, cells in the former case develop compensatory mechanisms to rectify the deficiencies caused by the inhibition of the siRNA-targeted endocytic pathway. This adaptation often manifests as upregulation of alternate endocytic pathways, which seems reasonable given that the surface area of cells do not change drastically over the course of the siRNA-induced effect. Evidence of this “cross-regulation” (Mayor and Pagano 2007) between different endocytic pathways can be gathered from the studies of Schmid et al., which showed upregulation of fluid-phase pinocytosis in dynamin mutants subjected to temperature dependent inhibition of clathrin-mediated endocytosis (Damke, Baba et al. 1995).

In our study, siRNA-induced inhibition of one endocytic mechanism may induce upregulation of alternate pathways that facilitate pDNA uptake during electrotransfection. Pharmacological inhibitors, on the other hand, produce an immediate, transient effect which does not allow cells sufficient time to adapt or develop the same compensatory mechanisms, thereby resulting in the more pronounced effects on electrotransfection efficiency seen. Alternatively, because of the questionable specificity of the pharmacological approach discussed earlier, the dramatic reductions in eTE may also be attributed to unintended effects of the drug treatment on alternate endocytic pathways or non-endocytic molecules/mechanisms that affect electrotransfection efficiency.

4.5 Conclusions

We first proposed endocytosis to play a role in electric field-mediated pDNA uptake in a seminal paper that investigated the effects of endocytic inhibitors and siRNA knockdown of dynamin on electrotransfection efficiency in B16.F10, a murine melanoma cell line (Wu and Yuan). This follow-up study used the same combination strategy of pharmacological agents and RNA interference to probe the endocytic pathways involved in electrotransfection of two different cell lines, HT29 (human colon adenocarcinoma) and NHDFs (normal, adult human dermal fibroblasts). The combined findings of this study and the previous paper show that different endocytic pathways

are recruited during electrotransfection in a cell line-dependent manner. Furthermore, a single or multiple endocytic pathway(s) may participate in electrically-induced internalization of DNA, depending on the cell line. It is known that different endocytic pathways result in different intracellular destinations, with some leading to the perinuclear region, resulting in subsequent entry into the nucleus and gene expression, while others ultimately end in lysosomal degradation of their cargo (Luo and Saltzman 2000). Thus, among many other factors, the specific endocytic pathway(s) recruited for pDNA uptake and subsequent intracellular transport may dictate the transfection efficiency achieved by electrotransfection for a particular cell line. Further evidence to support our hypothesis that endocytosis facilitates the uptake of pDNA during electrotransfection can be gathered from the work of Rosazza et al., which showed colocalization of fluorescently-labeled pDNA with actin patches upon electric field exposure and reduction in gene expression as a result of actin depolymerization treatment prior to pulse application (Rosazza, Escoffre et al. 2011). The actin cytoskeleton being necessary for the invagination, budding, and early vesicular transport of endocytic vesicles for multiple pathways, including macropinocytosis and caveolae-dependent endocytosis, Rosazza's findings corroborate our results in suggesting that endocytic pathways are involved in electric field-mediated DNA uptake.

Chapter 5

Future Works

5.1 Visualization of the Effect of Endocytic Inhibition on Electric Field-mediated pDNA Uptake and Intracellular Distribution

In the studies outlined in Chapter 3 and 4, electrotransfection efficiency (as measured by GFP expression) was used as a means of quantifying the effect of endocytic inhibition, either via pharmacological agents or siRNA knockdown of endocytic proteins, on transmembrane and intracellular transport of pDNA. Although transfection efficiency is dependent upon pDNA transport across these physiological barriers, it is also impacted by barriers further downstream such as transport across the nuclear envelope and the efficiency of gene expression of the reporter plasmid once inside the nucleus. Thus, measuring transfection efficiency as a secondary effect of pDNA transport across the cell membrane and cytosol, may result in misleading conclusions regarding the role and impact of endocytic pathways.

Although the transfection studies described in this dissertation do provide compelling evidence in implicating endocytic pathways, a better, more conclusive approach would be to observe the direct effect of endocytosis on pDNA uptake and intracellular distribution following electric field pulse treatment.

Fluorescence microscopy of fluorescently labeled plasmid DNA can be used to verify reduced DNA uptake as a result of endocytic inhibition, after pulsed, electric field application. Based on experience, fluorescent DNA intercalating dyes such as YOYO-1 nucleic acid stain (Invitrogen) has proven to be unsuitable for these studies due to the influx of free dye molecules into cells during electric field application, which leads to high background fluorescence as a result of nonspecific binding to intracellular organelles/membrane and staining of cell nuclei. Covalent DNA labels such as the Label-IT™-Rhodamine fluorescent dye (Mirus Corp) serve this purpose better as free dye molecules are filtered from the DNA solution prior to use and the covalent nature of the label prevents dissociation of bound dye molecules from the plasmid DNA. Cells would be subjected to endocytic inhibition via either pharmacological agents or siRNA knockdown, in the same manner as for the electrotransfection studies. Instead of electrotransfecting cells with GFP-encoding plasmid and measuring transfection efficiency 24 hours later, cells would be electrotransfected with fluorescently-tagged plasmid and observed under a fluorescent, confocal microscope shortly afterwards, to track the uptake and intracellular distribution of pDNA. Qualitative visual comparison and quantitative image analysis can be used to confirm reductions in the internalization and intracellular accumulation of fluorescent pDNA in the endocytosis-inhibited groups.

5.2 Visualization of Colocalization of Fluorescently-labeled Endocytic Vesicles and fluorescently-tagged plasmid DNA Following EFMGD

Endocytosis can be further implicated in electric-field mediated DNA delivery via colocalization studies of fluorescently-labeled endocytic vesicles with fluorescently tagged plasmid DNA. Fluorescent tagging of pDNA is described above in Section 5.1. Fluorescent labeling of endocytic vesicles can be accomplished by using a general fluorescent membrane stain such as FM4-64FX (Invitrogen), an amphipathic dye that embeds into the outer leaflet of the plasma membrane, cannot diffuse across the membrane, and can only be internalized via the formation and scission of endocytic vesicles. Based on experience, however, this stain also causes diffuse background staining of the entire intracellular milieu (most likely due to fusion of the labeled vesicles with other intracellular membranous organelles/compartments such as the ER, Golgi Apparatus), which obscures visualization of the actual, labeled endocytic vesicles. A better strategy would be more specific, targeted labeling of endocytic vesicles using fluorescent fusion proteins conjugated to different endocytic proteins (ie. GFP-clathrin and GFP-caveolin). Different endocytic pathways can be tagged by different fluorescent proteins (e.g. green fluorescent protein(GFP)/clathrin and blue fluorescent protein(BFP)/caveolin fusion proteins) , to permit easy identification of the specific endocytic pathway involved in uptake of the fluorescently-labeled DNA based on the color of the colocalized spots. In cell lines where more than one pathway is recruited

(e.g. B16.F10 and NHDF, based on our studies), valuable quantitative information regarding the individual contribution of each pathway to overall DNA uptake can be determined from image analysis of these colocalization micrographs.

5.3 Pulsed Electric Field Parameter-dependent Recruitment of Endocytic Pathway(s)

It is known that electrotransfection efficiency of EFMGD is highly dependent on the electrotransfection parameters of field strength magnitude, pulse number, pulse duration, and frequency, which must be empirically optimized for each cell line. The exact mechanism in which these electric field parameters dictate electrotransfection efficiency is uncertain. As described previously in Chapter, 2, the magnitude of the electric field strength is crucial in inducing a transmembrane voltage potential difference that exceeds a critical threshold value, resulting in permeabilization of the membrane regions facing both electrodes. This critical threshold is crucial for not only membrane permeabilization to permit the influx of external, small molecules but also for DNA electrotransfection, since subthreshold values do not result in transfection. In addition to 'porating' or permeabilizing the cell membrane, it has been proposed that pulsed, electric field may also facilitate cell transfection by generating an electrophoretic effect on the polyanionic pDNA to help drive its translocation across the cell membrane and possibly also its intracellular transport. This has been investigated in both in vitro and in vivo studies.

However, the possibility may exist that different pulsed electric field parameters lead to different transfection efficiencies, not by the aforementioned mechanisms, but by inducing and/or upregulating different endocytic pathways. This hypothesis is based on an interesting, unexpected observation made during pulse treatment optimization for HT29 cells during the pharmacological studies. A variety of different electric field magnitude, pulse duration, and pulse number combinations were tested on the drug-treated cells, in attempt to maximize transfection efficiency while minimizing loss to cell viability. Whether the endocytic drug treatment produced an effect on electrotransfection efficiency (eTE) appeared to vary depending on the particular pulse treatment regimen used. The effect of chlorpromazine and genistein treatment on eTE for different pulse treatments is shown in **Figure 5.1**. Amiloride treatment was not tested.

As shown in **Figure 5.1**, chlorpromazine treatment exhibits a reduction in eTE when cells were subjected to pulse treatments of 240V, 5ms, 6 Pulses and 240V, 5ms, 8 Pulses but no change in eTE for the other pulse treatments tested. Genistein treatment does not appear to have any substantial effect on eTE for any of the three pulsing regimens tested. These preliminary findings seem to suggest that different electric field parameters may lead to the recruitment of different endocytic pathways for electric field-mediated DNA internalization. It is conceivable that since different endocytic pathways result in different intracellular trafficking, processing, and destinations of

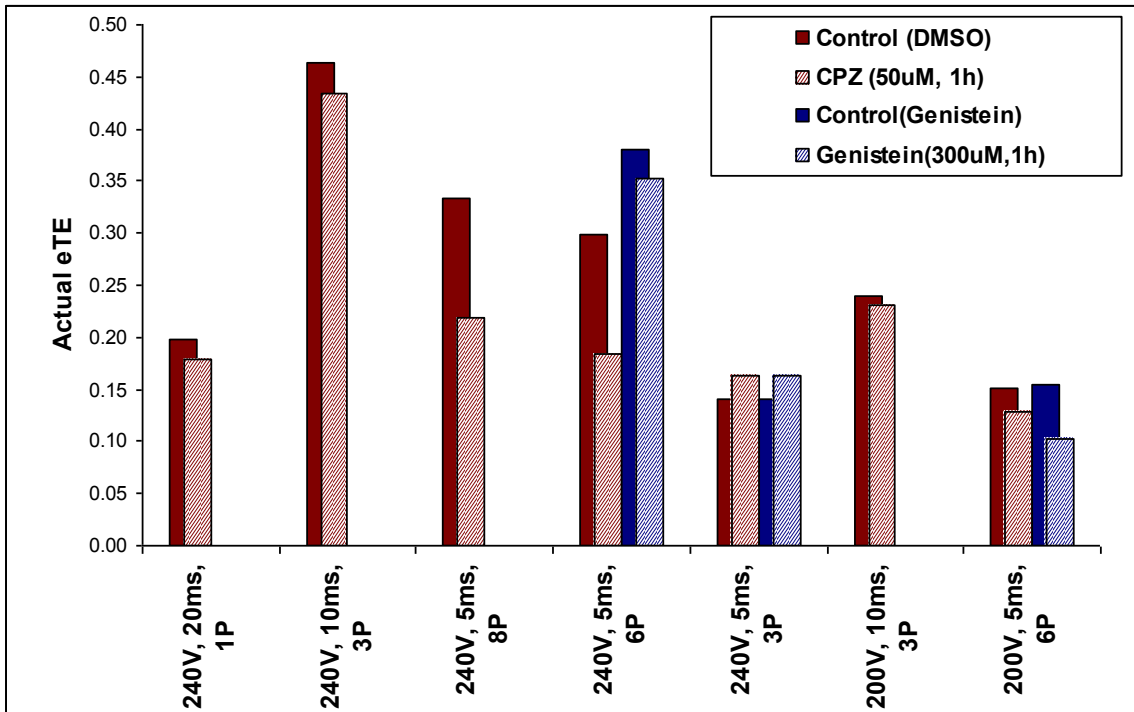


Figure 5.1: Effect of chlorpromazine (50 μ M, 1h) and genistein (300 μ M, 1h) treatment on electrotransfection efficiency of HT29 for different electric field pulse regimens. N=2-3 trials for all groups except for '240V,5ms,6P' group (N=5-6 trials)

their cargo, transfection efficiency may be highly dependent on the mechanism of internalization (Rejman, Oberle et al. 2004). Thus, depending on the pathway or combination of pathways recruited for a given pulsing regimen, the overall transfection efficiency achieved could be a weighted average of the percentage of pDNA internalized via each of the pathways and the efficiency of gene delivery and expression for each of these pathways.

To further investigate this potential phenomenon, a more systematic study needs be conducted in which each electric field parameter (magnitude, pulse duration, pulse

number, frequency) is varied while keeping the other parameters constant, in order to determine which parameter(s) play(s) the most crucial role in dictating recruitment of different endocytic pathways. Additional pharmacological inhibitors with alternate mechanisms of inhibiting macropinocytosis, clathrin-mediated and caveolae-dependent endocytosis should be tested to provide redundancy and ensure that the results seen are not attributed to nonspecific, side effects of the endocytic drugs used in these studies. siRNA silencing is not recommended for these particular studies due to the likelihood of cells developing compensatory mechanisms or upregulating of alternate endocytic pathways that would mask the true impact of the inhibited pathway on observed electrotransfection efficiency.

References

- Aihara, H. and J. Miyazaki (1998). "Gene transfer into muscle by electroporation in vivo." Nature biotechnology **16**(9): 867-870.
- Amyere, M., B. Payraastre, et al. (2000). "Constitutive macropinocytosis in oncogene-transformed fibroblasts depends on sequential permanent activation of phosphoinositide 3-kinase and phospholipase C." Mol Biol Cell **11**(10): 3453-67.
- Angelova, M. I., N. Hristova, et al. (1999). "DNA-induced endocytosis upon local microinjection to giant unilamellar cationic vesicles." Eur Biophys J **28**(2): 142-50.
- Angelova, M. I. and I. Tsoneva (1999). "Interactions of DNA with giant liposomes." Chem Phys Lipids **101**(1): 123-37.
- Antov, Y., A. Barbul, et al. (2005). "Electroendocytosis: exposure of cells to pulsed low electric fields enhances adsorption and uptake of macromolecules." Biophys J **88**(3): 2206-23.
- Artalejo, C. R., J. R. Henley, et al. (1995). "Rapid endocytosis coupled to exocytosis in adrenal chromaffin cells involves Ca²⁺, GTP, and dynamin but not clathrin." Proc Natl Acad Sci U S A **92**(18): 8328-32.
- Bardor, M., D. H. Nguyen, et al. (2005). "Mechanism of uptake and incorporation of the non-human sialic acid N-glycolylneuraminic acid into human cells." J Biol Chem **280**(6): 4228-37.
- Bermudez, L. E. and L. S. Young (1994). "Factors affecting invasion of HT-29 and HEp-2 epithelial cells by organisms of the Mycobacterium avium complex." Infect Immun **62**(5): 2021-6.
- Bier, M., S. M. Hammer, et al. (1999). "Kinetics of sealing for transient electropores in isolated mammalian skeletal muscle cells." Bioelectromagnetics **20**(3): 194-201.
- Bodwell, J., F. Swiff, et al. (1999). "Long duration electroporation for achieving high level expression of glucocorticoid receptors in mammalian cell lines." J Steroid Biochem Mol Biol **68**(1-2): 77-82.

- Bureau, M. F., J. Gehl, et al. (2000). "Importance of association between permeabilization and electrophoretic forces for intramuscular DNA electrotransfer." Biochimica Et Biophysica Acta-General Subjects **1474**(3): 353-359.
- Bureau, M. F., S. Naimi, et al. (2004). "Intramuscular plasmid DNA electrotransfer: biodistribution and degradation." Biochim Biophys Acta **1676**(2): 138-48.
- Calder, P. C. and P. Yaqoob (2007). "Lipid rafts--composition, characterization, and controversies." J Nutr **137**(3): 545-7.
- Campbell, S. M., S. M. Crowe, et al. (2001). "Lipid rafts and HIV-1: from viral entry to assembly of progeny virions." J Clin Virol **22**(3): 217-27.
- Cemazar, M., G. Sersa, et al. (2002). "Effective gene transfer to solid tumors using different nonviral gene delivery techniques: Electroporation, liposomes, and integrin-targeted vector." Cancer Gene Therapy **9**(4): 399-406.
- Chang, D. C. and T. S. Reese (1990). "Changes in membrane structure induced by electroporation as revealed by rapid-freezing electron microscopy." Biophys J **58**(1): 1-12.
- Chen, Y. and L. C. Norkin (1999). "Extracellular simian virus 40 transmits a signal that promotes virus enclosure within caveolae." Exp Cell Res **246**(1): 83-90.
- Chernomordik, L. V., A. V. Sokolov, et al. (1990). "Electrostimulated uptake of DNA by liposomes." Biochim Biophys Acta **1024**(1): 179-83.
- Collins, B. M., A. J. McCoy, et al. (2002). "Molecular architecture and functional model of the endocytic AP2 complex." Cell **109**(4): 523-35.
- Conner, S. D. and S. L. Schmid (2003). "Regulated portals of entry into the cell." Nature **422**(6927): 37-44.
- Cristiano, R. J. (1998). "Viral and non-viral vectors for cancer gene therapy." Anticancer Res **18**(5A): 3241-5.
- Cristiano, R. J., B. Xu, et al. (1998). "Viral and nonviral gene delivery vectors for cancer gene therapy." Cancer Detect Prev **22**(5): 445-54.

- Damke, H., T. Baba, et al. (1995). "Clathrin-independent pinocytosis is induced in cells overexpressing a temperature-sensitive mutant of dynamin." *J Cell Biol* **131**(1): 69-80.
- Dauty, E. and A. S. Verkman (2005). "Actin cytoskeleton as the principal determinant of size-dependent DNA mobility in cytoplasm." *Journal of Biological Chemistry* **280**(9): 7823-7828.
- Delteil, C., J. Teissie, et al. (2000). "Effect of serum on in vitro electrically mediated gene delivery and expression in mammalian cells." *Biochim Biophys Acta* **1467**(2): 362-8.
- Dimitrov, D. S. and A. E. Sowers (1990). "Membrane Electroporation - Fast Molecular-Exchange by Electroosmosis." *Biochimica Et Biophysica Acta* **1022**(3): 381-392.
- Doherty, G. J. and H. T. McMahon (2009). "Mechanisms of endocytosis." *Annu Rev Biochem* **78**: 857-902.
- Duguid, J., V. A. Bloomfield, et al. (1993). "Raman spectroscopy of DNA-metal complexes. I. Interactions and conformational effects of the divalent cations: Mg, Ca, Sr, Ba, Mn, Co, Ni, Cu, Pd, and Cd." *Biophys J* **65**(5): 1916-28.
- Elbashir, S. M., J. Harborth, et al. (2001). "Duplexes of 21-nucleotide RNAs mediate RNA interference in cultured mammalian cells." *Nature* **411**(6836): 494-8.
- Elferink, J. G. (1979). "Chlorpromazine inhibits phagocytosis and exocytosis in rabbit polymorphonuclear leukocytes." *Biochem Pharmacol* **28**(7): 965-8.
- Escoffre, J. M., T. Portet, et al. (2009). "What is (still not) known of the mechanism by which electroporation mediates gene transfer and expression in cells and tissues." *Mol Biotechnol* **41**(3): 286-95.
- Eynard, N., M. P. Rols, et al. (1997). "Electrotransformation pathways of procaryotic and eucaryotic cells: recent developments." *Bioelectrochemistry and Bioenergetics* **44**(1): 103-110.
- Faurie, C., M. Rebersek, et al. "Electro-mediated gene transfer and expression are controlled by the life-time of DNA/membrane complex formation." *J Gene Med* **12**(1): 117-25.

- Favard, C., D. S. Dean, et al. (2007). "Electrotransfer as a non viral method of gene delivery." Current Gene Therapy 7(1): 67-77.
- Francescu, A., S. Kakorin, et al. (2005). "Adsorption of DNA and electric fields decrease the rigidity of lipid vesicle membranes." Phys Chem Chem Phys 7(24): 4126-31.
- Francescu, A., K. Tonsing, et al. (2006). "Interfacial ternary complex DNA/Ca/lipids at anionic vesicle surfaces." Bioelectrochemistry 68(2): 158-70.
- Gabrielson, N. P. and D. W. Pack (2009). "Efficient polyethylenimine-mediated gene delivery proceeds via a caveolar pathway in HeLa cells." Journal of Controlled Release 136(1): 54-61.
- Gehl, J. (2003). "Electroporation: theory and methods, perspectives for drug delivery, gene therapy and research." Acta Physiol Scand 177(4): 437-47.
- Gekle, M., R. Freudinger, et al. (2001). "Inhibition of Na⁺-H⁺ exchanger-3 interferes with apical receptor-mediated endocytosis via vesicle fusion." J Physiol 531(Pt 3): 619-29.
- Gerdes, C. A., M. G. Castro, et al. (2000). "Strong promoters are the key to highly efficient, noninflammatory and noncytotoxic adenoviral-mediated transgene delivery into the brain in vivo." Mol Ther 2(4): 330-8.
- Glogauer, M., W. Lee, et al. (1993). "Induced endocytosis in human fibroblasts by electrical fields." Exp Cell Res 208(1): 232-40.
- Golzio, M., M. P. Rols, et al. (2004). "In vitro and in vivo electric field-mediated permeabilization, gene transfer, and expression." Methods 33(2): 126-35.
- Golzio, M., J. Teissié, et al. (2002). "Direct visualization at the single-cell level of electrically mediated gene delivery." Proceedings of the National Academy of Sciences 99(3): 1292-1297.
- Gratton, S. E. A., P. A. Ropp, et al. (2008). "The effect of particle design on cellular internalization pathways." Proceedings of the National Academy of Sciences of the United States of America 105(33): 11613-11618.

- Greenleaf, W. J., M. E. Bolander, et al. (1998). "Artificial cavitation nuclei significantly enhance acoustically induced cell transfection." Ultrasound in Medicine and Biology **24**(4): 587-595.
- Haas, K., K. Jensen, et al. (2002). "Targeted electroporation in *Xenopus* tadpoles in vivo - from single cells to the entire brain." Differentiation **70**(4-5): 148-154.
- Haberl, S., D. Miklavcic, et al. (2010). "Effect of Mg ions on efficiency of gene electrotransfer and on cell electroporabilization." Bioelectrochemistry **79**(2): 265-271.
- Harrison, R. L., B. J. Byrne, et al. (1998). "Electroporation-mediated gene transfer in cardiac tissue." Febs Letters **435**(1): 1-5.
- Hay, J. C. (2007). "Calcium: a fundamental regulator of intracellular membrane fusion?" EMBO Rep **8**(3): 236-40.
- Heller, L. C. and R. Heller (2006). "In vivo electroporation for gene therapy." Hum Gene Ther **17**(9): 890-7.
- Heller, L. C., M. J. Jaroszeski, et al. (2007). "Optimization of cutaneous electrically mediated plasmid DNA delivery using novel electrode." Gene Ther **14**(3): 275-80.
- Heller, L. C., K. Ugen, et al. (2005). "Electroporation for targeted gene transfer." Expert Opin Drug Deliv **2**(2): 255-68.
- Heller, R. (1995). "Treatment of cutaneous nodules using electrochemotherapy." J Fla Med Assoc **82**(2): 147-50.
- Heller, R., M. Jaroszeski, et al. (1996). "In vivo gene electroinjection and expression in rat liver." FEBS Lett **389**(3): 225-8.
- Heller, R., M. Jaroszeski, et al. (1996). "In vivo gene electroinjection and expression in rat liver." Febs Letters **389**(3): 225-228.
- Henshaw, J., B. Mossop, et al. "Enhancement of electric field-mediated gene delivery through pretreatment of tumors with a hyperosmotic mannitol solution." Cancer Gene Ther **18**(1): 26-33.

- Henshaw, J., B. Mossop, et al. (2008). "Relaxin treatment of solid tumors: effects on electric field-mediated gene delivery." Mol Cancer Ther 7(8): 2566-73.
- Henshaw, J. W. and F. Yuan (2008). "Field distribution and DNA transport in solid tumors during electric field-mediated gene delivery." J Pharm Sci 97(2): 691-711.
- Henshaw, J. W., D. A. Zaharoff, et al. (2007). "Electric field-mediated transport of plasmid DNA in tumor interstitium in vivo." Bioelectrochemistry 71(2): 233-42.
- Herz, J. and R. D. Gerard (1993). "Adenovirus-mediated transfer of low density lipoprotein receptor gene acutely accelerates cholesterol clearance in normal mice." Proc Natl Acad Sci U S A 90(7): 2812-6.
- Hinshaw, J. E. (2000). "Dynamin and its role in membrane fission." Annu Rev Cell Dev Biol 16: 483-519.
- Holen, T., M. Amarzguioui, et al. (2002). "Positional effects of short interfering RNAs targeting the human coagulation trigger Tissue Factor." Nucleic Acids Res 30(8): 1757-66.
- Hristova, N. I., I. Tsoneva, et al. (1997). "Sphingosine-mediated electroporative DNA transfer through lipid bilayers." FEBS Lett 415(1): 81-6.
- Hsu, T. and S. Mitragotri "Delivery of siRNA and other macromolecules into skin and cells using a peptide enhancer." Proc Natl Acad Sci U S A 108(38): 15816-21.
- Huber, P. E. and P. Pfisterer (2000). "In vitro and in vivo transfection of plasmid DNA in the Dunning prostate tumor R3327-AT1 is enhanced by focused ultrasound." Gene Therapy 7(17): 1516-1525.
- Ivanov, A. I. (2008). "Pharmacological inhibition of endocytic pathways: is it specific enough to be useful?" Methods Mol Biol 440: 15-33.
- Ivanov, A. I., A. Nusrat, et al. (2004). "Endocytosis of epithelial apical junctional proteins by a clathrin-mediated pathway into a unique storage compartment." Mol Biol Cell 15(1): 176-88.
- Jenne, L., G. Schuler, et al. (2001). "Viral vectors for dendritic cell-based immunotherapy." Trends Immunol 22(2): 102-7.

- Ji, J., M. Wernli, et al. (2003). "Enhanced gene silencing by the application of multiple specific small interfering RNAs." FEBS Lett **552**(2-3): 247-52.
- Kartenbeck, J., H. Stukenbrok, et al. (1989). "Endocytosis of simian virus 40 into the endoplasmic reticulum." J Cell Biol **109**(6 Pt 1): 2721-9.
- Khalil, I. A., K. Kogure, et al. (2006). "Uptake pathways and subsequent intracellular trafficking in nonviral gene delivery." Pharmacol Rev **58**(1): 32-45.
- Kim, H. J., J. F. Greenleaf, et al. (1996). "Ultrasound-mediated transfection of mammalian cells." Human Gene Therapy **7**(11): 1339-1346.
- Kinosita, K., Jr. and T. Y. Tsong (1977). "Voltage-induced pore formation and hemolysis of human erythrocytes." Biochim Biophys Acta **471**(2): 227-42.
- Kirkham, M. and R. G. Parton (2005). "Clathrin-independent endocytosis: new insights into caveolae and non-caveolar lipid raft carriers." Biochim Biophys Acta **1746**(3): 349-63.
- Kleinchin, V. A., Sudkarev, S.I., Serov, S.M., Chernomordik, L.V, Chizmadzhev Yu, A (1991). "Electrically induced DNA uptake by cells is a fast process involving DNA electrophoresis." Biophysical journal **60**(4): 804-811.
- Koivusalo, M., C. Welch, et al. (2010). "Amiloride inhibits macropinocytosis by lowering submembranous pH and preventing Rac1 and Cdc42 signaling (vol 188, pg 547, 2010)." Journal of Cell Biology **189**(2).
- Kojic, L. D., S. M. Wiseman, et al. (2008). "Raft-dependent endocytosis of autocrine motility factor/phosphoglucose isomerase: a potential drug delivery route for tumor cells." PLoS One **3**(10): e3597.
- Krassowska, W. and P. D. Filev (2007). "Modeling electroporation in a single cell." Biophys J **92**(2): 404-17.
- Krotz, F., H. Y. Sohn, et al. (2003). "Magnetofection potentiates gene delivery to cultured endothelial cells." Journal of Vascular Research **40**(5): 425-434.
- Kurzchalia, T. V. and R. G. Parton (1999). "Membrane microdomains and caveolae." Curr Opin Cell Biol **11**(4): 424-31.

- Lagana, A., J. Vadnais, et al. (2000). "Regulation of the formation of tumor cell pseudopodia by the Na(+)/H(+) exchanger NHE1." J Cell Sci **113 (Pt 20)**: 3649-62.
- Lakshmipathy, U., B. Pelacho, et al. (2004). "Efficient transfection of embryonic and adult stem cells." Stem Cells **22(4)**: 531-543.
- Lauer, U., E. Burgelt, et al. (1997). "Shock wave permeabilization as a new gene transfer method." Gene Therapy **4(7)**: 710-715.
- Lechardeur, D., K. J. Sohn, et al. (1999). "Metabolic instability of plasmid DNA in the cytosol: a potential barrier to gene transfer." Gene Ther **6(4)**: 482-97.
- Li, H., S. T. Chan, et al. (1997). "Transfection of rat brain cells by electroporation." J Neurosci Methods **75(1)**: 29-32.
- Liu, F., S. Heston, et al. (2006). "Mechanism of in vivo DNA transport into cells by electroporation: electrophoresis across the plasma membrane may not be involved." J Gene Med **8(3)**: 353-61.
- Liu, F., Y. Song, et al. (1999). "Hydrodynamics-based transfection in animals by systemic administration of plasmid DNA." Gene Ther **6(7)**: 1258-66.
- Lohr, F., D. Y. Lo, et al. (2001). "Effective tumor therapy with plasmid-encoded cytokines combined with in vivo electroporation." Cancer Res **61(8)**: 3281-4.
- Lukacs, G. L., P. Haggie, et al. (2000). "Size-dependent DNA mobility in cytoplasm and nucleus." J Biol Chem **275(3)**: 1625-9.
- Luo, D. and W. M. Saltzman (2000). "Synthetic DNA delivery systems." Nat Biotechnol **18(1)**: 33-7.
- Marjomaki, V., V. Pietiainen, et al. (2002). "Internalization of echovirus 1 in caveolae." J Virol **76(4)**: 1856-65.
- Mayor, S. and R. E. Pagano (2007). "Pathways of clathrin-independent endocytosis." Nat Rev Mol Cell Biol **8(8)**: 603-12.
- Mehier-Humbert, S. and R. H. Guy (2005). "Physical methods for gene transfer: improving the kinetics of gene delivery into cells." Adv Drug Deliv Rev **57(5)**: 733-53.

- Meier, O., K. Boucke, et al. (2002). "Adenovirus triggers macropinocytosis and endosomal leakage together with its clathrin-mediated uptake." J Cell Biol **158**(6): 1119-31.
- Meier, O. and U. F. Greber (2003). "Adenovirus endocytosis." J Gene Med **5**(6): 451-62.
- Mellman, I. (1996). "Endocytosis and molecular sorting." Annu Rev Cell Dev Biol **12**: 575-625.
- Mengistu, D. H., K. Bohinc, et al. (2009). "Binding of DNA to zwitterionic lipid layers mediated by divalent cations." J Phys Chem B **113**(36): 12277-82.
- Michel, M. R., M. Elgizoli, et al. (1988). "Diffusion loading conditions determine recovery of protein synthesis in electroporated P3X63Ag8 cells." Experientia **44**(3): 199-203.
- Miller, D. L., S. P. Bao, et al. (1999). "Ultrasonic enhancement of gene transfection in murine melanoma tumors." Ultrasound in Medicine and Biology **25**(9): 1425-1430.
- Miller, D. L., S. V. Pislaru, et al. (2002). "Sonoporation: mechanical DNA delivery by ultrasonic cavitation." Somat Cell Mol Genet **27**(1-6): 115-34.
- Mir, L. M., M. F. Bureau, et al. (1999). "High-efficiency gene transfer into skeletal muscle mediated by electric pulses." Proceedings of the National Academy of Sciences of the United States of America **96**(8): 4262-4267.
- Monier, S., R. G. Parton, et al. (1995). "VIP21-caveolin, a membrane protein constituent of the caveolar coat, oligomerizes in vivo and in vitro." Mol Biol Cell **6**(7): 911-27.
- Nabi, I. R. and P. U. Le (2003). "Caveolae/raft-dependent endocytosis." Journal of Cell Biology **161**(4): 673-677.
- Nakashima, S., Y. Matsuyama, et al. (2005). "Highly efficient transfection of human marrow stromal cells by nucleofection." Transplantation Proceedings **37**(5): 2290-2292.
- Nemeth, Z. H., E. A. Deitch, et al. (2002). "Na⁺/H⁺ exchanger blockade inhibits enterocyte inflammatory response and protects against colitis." American Journal of Physiology-Gastrointestinal and Liver Physiology **283**(1): G122-G132.

- Neumann, E., S. Kakorin, et al. (1996). "Calcium-mediated DNA adsorption to yeast cells and kinetics of cell transformation by electroporation." Biophys J **71**(2): 868-77.
- Neumann, E., M. Schaefer-Ridder, et al. (1982). "Gene transfer into mouse lyoma cells by electroporation in high electric fields." EMBO J **1**(7): 841-5.
- Nichols, B. J. and J. Lippincott-Schwartz (2001). "Endocytosis without clathrin coats." Trends in Cell Biology **11**(10): 406-412.
- Nishi, T., K. Yoshizato, et al. (1996). "High-efficiency in vivo gene transfer using intraarterial plasmid DNA injection following in vivo electroporation." Cancer Res **56**(5): 1050-5.
- O'Brien, J. and S. C. R. Lummis (2004). "Biolistic and diolistic transfection: using the gene gun to deliver DNA and lipophilic dyes into mammalian cells." Methods **33**(2): 121-125.
- Ogiso, T., M. Iwaki, et al. (1981). "Fluidity of human erythrocyte membrane and effect of chlorpromazine on fluidity and phase separation of membrane." Biochim Biophys Acta **649**(2): 325-35.
- Pack, D. W., A. S. Hoffman, et al. (2005). "Design and development of polymers for gene delivery." Nat Rev Drug Discov **4**(7): 581-93.
- Papatheodorou, P., C. Zamboglou, et al. "Clostridial glucosylating toxins enter cells via clathrin-mediated endocytosis." PLoS One **5**(5): e10673.
- Parton, R. G., B. Joggerst, et al. (1994). "Regulated Internalization of Caveolae." Journal of Cell Biology **127**(5): 1199-1215.
- Pavlin, M., M. Kanduser, et al. (2009). "Analysis of Mechanisms Involved in Gene Electrotransfer - Theoretical and an in Vitro Study." World Congress on Medical Physics and Biomedical Engineering, Vol 25, Pt 13 **25**(13): 158-161.
- Pelkmans, L., T. Burli, et al. (2004). "Caveolin-stabilized membrane domains as multifunctional transport and sorting devices in endocytic membrane traffic." Cell **118**(6): 767-80.
- Pelkmans, L. and A. Helenius (2002). "Endocytosis via caveolae." Traffic **3**(5): 311-20.

- Pelkmans, L., J. Kartenbeck, et al. (2001). "Caveolar endocytosis of simian virus 40 reveals a new two-step vesicular-transport pathway to the ER." Nat Cell Biol **3**(5): 473-83.
- Pelkmans, L., D. Puntener, et al. (2002). "Local actin polymerization and dynamin recruitment in SV40-induced internalization of caveolae." Science **296**(5567): 535-9.
- Phez, E., C. Faurie, et al. (2005). "New insights in the visualization of membrane permeabilization and DNA/membrane interaction of cells submitted to electric pulses." Biochim Biophys Acta **1724**(3): 248-54.
- Pike, L. J. (2004). "Lipid rafts: heterogeneity on the high seas." Biochem J **378**(Pt 2): 281-92.
- Plank, C., U. Schillinger, et al. (2003). "The magnetofection method: using magnetic force to enhance gene delivery." Biol Chem **384**(5): 737-47.
- Pouton, C. W., K. M. Wagstaff, et al. (2007). "Targeted delivery to the nucleus." Adv Drug Deliv Rev **59**(8): 698-717.
- Prausnitz, M. R., J. D. Corbett, et al. (1995). "Millisecond measurement of transport during and after an electroporation pulse." Biophys J **68**(5): 1864-70.
- Puri, V., R. Watanabe, et al. (2001). "Clathrin-dependent and -independent internalization of plasma membrane sphingolipids initiates two Golgi targeting pathways." J Cell Biol **154**(3): 535-47.
- Rea, J. C., R. F. Gibly, et al. (2009). "Engineering surfaces for substrate-mediated gene delivery using recombinant proteins." Biomacromolecules **10**(10): 2779-86.
- Rejman, J., A. Bragonzi, et al. (2005). "Role of clathrin- and caveolae-mediated endocytosis in gene transfer mediated by lipo- and polyplexes." Mol Ther **12**(3): 468-74.
- Rejman, J., M. Conese, et al. (2006). "Gene transfer by means of lipo- and polyplexes: role of clathrin and caveolae-mediated endocytosis." J Liposome Res **16**(3): 237-47.

- Rejman, J., V. Oberle, et al. (2004). "Size-dependent internalization of particles via the pathways of clathrin- and caveolae-mediated endocytosis." Biochem J **377**(Pt 1): 159-69.
- Robbins, P. D. and S. C. Ghivizzani (1998). "Viral vectors for gene therapy." Pharmacol Ther **80**(1): 35-47.
- Rols, M., C. Delteil, et al. (1998). "In vivo electrically mediated protein and gene transfer in murine melanoma." Nature biotechnology **16**(2): 168-171.
- Rols, M. P., P. Femenia, et al. (1995). "Long-lived macropinocytosis takes place in electropermeabilized mammalian cells." Biochem Biophys Res Commun **208**(1): 26-35.
- Rosazza, C., J. M. Escoffre, et al. (2011). "The Actin Cytoskeleton Has an Active Role in the Electrotransfer of Plasmid DNA in Mammalian Cells." Molecular Therapy **19**(5): 913-921.
- Roux, A., K. Uyhazi, et al. (2006). "GTP-dependent twisting of dynamin implicates constriction and tension in membrane fission." Nature **441**(7092): 528-31.
- Sabelnikov, A. G. (1994). "Nucleic-Acid Transfer through Cell-Membranes - Towards the Underlying Mechanisms." Progress in Biophysics & Molecular Biology **62**(2): 119-152.
- Saovapakhiran, A., A. D'Emanuele, et al. (2009). "Surface modification of PAMAM dendrimers modulates the mechanism of cellular internalization." Bioconjug Chem **20**(4): 693-701.
- Satkauskas, S., M. F. Bureau, et al. (2001). "Slow accumulation of plasmid in muscle cells: supporting evidence for a mechanism of DNA uptake by receptor-mediated endocytosis." Mol Ther **4**(4): 317-23.
- Scherer, F., M. Anton, et al. (2002). "Magnetofection: enhancing and targeting gene delivery by magnetic force in vitro and in vivo." Gene Therapy **9**(2): 102-109.
- Sharma, D. K., J. C. Brown, et al. (2004). "Selective stimulation of caveolar endocytosis by glycosphingolipids and cholesterol." Mol Biol Cell **15**(7): 3114-22.

- Sieczkarski, S. B. and G. R. Whittaker (2002). "Influenza virus can enter and infect cells in the absence of clathrin-mediated endocytosis." Journal of Virology **76**(20): 10455-10464.
- Spassova, M., I. Tsoneva, et al. (1994). "Dip patch clamp currents suggest electrodiffusive transport of the polyelectrolyte DNA through lipid bilayers." Biophys Chem **52**(3): 267-74.
- Strayer, D. S. (1998). "Viral vectors for gene therapy: past, present and future." Drug News Perspect **11**(5): 277-86.
- Stuart, A. D., H. E. Eustace, et al. (2002). "A novel cell entry pathway for a DAF-using human enterovirus is dependent on lipid rafts." J Virol **76**(18): 9307-22.
- Sugar, I. P. and E. Neumann (1984). "Stochastic model for electric field-induced membrane pores. Electroporation." Biophys Chem **19**(3): 211-25.
- Sukharev, S. I., Kleinchin, V.A., Serov, S.M., Chernomordik, L.V., Chizmadzhev Yu, A (1992). "Electroporation and electrophoretic DNA transfer in cells. The effect of DNA interaction with electropores." Biophysical journal **63**(5): 1320-1327.
- Sun, P., H. Yamamoto, et al. (2003). "Small GTPase Rah/Rab34 is associated with membrane ruffles and macropinosomes and promotes macropinosome formation." J Biol Chem **278**(6): 4063-71.
- Swanson, J. A. and C. Watts (1995). "Macropinocytosis." Trends Cell Biol **5**(11): 424-8.
- Sweitzer, S. M. and J. E. Hinshaw (1998). "Dynamin undergoes a GTP-dependent conformational change causing vesiculation." Cell **93**(6): 1021-9.
- Tagawa, A., A. Mezzacasa, et al. (2005). "Assembly and trafficking of caveolar domains in the cell: caveolae as stable, cargo-triggered, vesicular transporters." J Cell Biol **170**(5): 769-79.
- Tarek, M. (2005). "Membrane electroporation: A molecular dynamics simulation." Biophysical journal **88**(6): 4045-4053.
- Tata, D. B., F. Dunn, et al. (1997). "Selective clinical ultrasound signals mediate differential gene transfer and expression in two human prostate cancer cell lines:

LnCap and PC-3." Biochemical and Biophysical Research Communications **234**(1): 64-67.

Teissie, J., M. Golzio, et al. (2005). "Mechanisms of cell membrane electropermeabilization: a minireview of our present (lack of ?) knowledge." Biochim Biophys Acta **1724**(3): 270-80.

Teissie, J. and M. P. Rols (1993). "An experimental evaluation of the critical potential difference inducing cell membrane electropermeabilization." Biophys J **65**(1): 409-13.

Thomsen, P., K. Roepstorff, et al. (2002). "Caveolae are highly immobile plasma membrane microdomains, which are not involved in constitutive endocytic trafficking." Mol Biol Cell **13**(1): 238-50.

Toneguzzo, F., A. Keating, et al. (1988). "Electric field-mediated gene transfer: characterization of DNA transfer and patterns of integration in lymphoid cells." Nucleic Acids Res **16**(12): 5515-32.

van der Aa, M. A. E. M., U. S. Huth, et al. (2007). "Cellular uptake of cationic polymer-DNA complexes via caveolae plays a pivotal role in gene transfection in COS-7 cells." Pharmaceutical Research **24**(8): 1590-1598.

Vaughan, E. E. and D. A. Dean (2006). "Intracellular trafficking of plasmids during transfection is mediated by microtubules." Mol Ther **13**(2): 422-8.

Vaughan, E. E., R. C. Geiger, et al. (2008). "Microtubule Acetylation Through HDAC6 Inhibition Results in Increased Transfection Efficiency." Molecular Therapy **16**(11): 1841-1847.

Vercauteren, D., R. E. Vandenbroucke, et al. (2009). "The Use of Inhibitors to Study Endocytic Pathways of Gene Carriers: Optimization and Pitfalls." Mol Ther.

Wadia, J. S., R. V. Stan, et al. (2004). "Transducible TAT-HA fusogenic peptide enhances escape of TAT-fusion proteins after lipid raft macropinocytosis." Nat Med **10**(3): 310-5.

Wang, L. H., K. G. Rothberg, et al. (1993). "Mis-assembly of clathrin lattices on endosomes reveals a regulatory switch for coated pit formation." J Cell Biol **123**(5): 1107-17.

- Watanabe, S., M. Hirose, et al. (1988). "Calmodulin antagonists inhibit the phagocytic activity of cultured Kupffer cells." Lab Invest **59**(2): 214-8.
- Weaver, J. C. (1993). "Electroporation: a general phenomenon for manipulating cells and tissues." J Cell Biochem **51**(4): 426-35.
- Weaver, J. C. and Y. A. Chizmadzhev (1996). "Theory of electroporation: A review." Bioelectrochemistry and Bioenergetics **41**(2): 135-160.
- Wells, A., M. F. Ware, et al. (1999). "Shaping up for shipping out: PLCgamma signaling of morphology changes in EGF-stimulated fibroblast migration." Cell Motil Cytoskeleton **44**(4): 227-33.
- Wells, C. L., R. P. Jechorek, et al. (1999). "The isoflavone genistein inhibits internalization of enteric bacteria by cultured Caco-2 and HT-29 enterocytes." J Nutr **129**(3): 634-40.
- Wells, J. M., L. H. Li, et al. (2000). "Electroporation-enhanced gene delivery in mammary tumors." Gene Therapy **7**(7): 541-547.
- Werling, D., J. C. Hope, et al. (1999). "Involvement of caveolae in the uptake of respiratory syncytial virus antigen by dendritic cells." J Leukoc Biol **66**(1): 50-8.
- Williams, R. S., S. A. Johnston, et al. (1991). "Introduction of Foreign Genes into Tissues of Living Mice by DNA-Coated Microprojectiles." Proceedings of the National Academy of Sciences of the United States of America **88**(7): 2726-2730.
- Williams, S. K. and R. C. Wagner (1981). "Regulation of micropinocytosis in capillary endothelium by multivalent cations." Microvasc Res **21**(2): 175-82.
- Wiranowska, M., L. O. Colina, et al. "Clathrin-mediated entry and cellular localization of chlorotoxin in human glioma." Cancer Cell Int **11**(1): 27.
- Wolf, H., M. P. Rols, et al. (1994). "Control by pulse parameters of electric field-mediated gene transfer in mammalian cells." Biophys J **66**(2 Pt 1): 524-31.
- Wong, A. W., S. J. Scales, et al. (2007). "DNA internalized via caveolae requires microtubule-dependent, Rab7-independent transport to the late endocytic pathway for delivery to the nucleus." J Biol Chem **282**(31): 22953-63.

- Wu, M. and F. Yuan "Membrane binding of plasmid DNA and endocytic pathways are involved in electrotransfection of mammalian cells." PLoS One **6**(6): e20923.
- Xie, T. D. and T. Y. Tsong (1993). "Study of mechanisms of electric field-induced DNA transfection. V. Effects of DNA topology on surface binding, cell uptake, expression, and integration into host chromosomes of DNA in the mammalian cell." Biophys J **65**(4): 1684-9.
- Yang, N. S., J. Burkholder, et al. (1990). "In vivo and in vitro gene transfer to mammalian somatic cells by particle bombardment." Proc Natl Acad Sci U S A **87**(24): 9568-72.
- Zaharoff, D. A., J. W. Henshaw, et al. (2008). "Mechanistic analysis of electroporation-induced cellular uptake of macromolecules." Exp Biol Med (Maywood) **233**(1): 94-105.
- Zefirov, A. L., M. M. Abdrakhmanov, et al. (2006). "The role of extracellular calcium in exo- and endocytosis of synaptic vesicles at the frog motor nerve terminals." Neuroscience **143**(4): 905-10.
- Zhang, G., X. Gao, et al. (2004). "Hydroporation as the mechanism of hydrodynamic delivery." Gene Therapy **11**(8): 675-682.
- Zhang, G. F., V. Budker, et al. (1999). "High levels of foreign gene expression in hepatocytes after tail vein injections of naked plasmid DNA." Human Gene Therapy **10**(10): 1735-1737.
- Zhang, G. F., D. Vargo, et al. (1997). "Expression of naked plasmid DNA injected into the afferent and efferent vessels of rodent and dog livers." Human Gene Therapy **8**(15): 1763-1772.
- Zhang, Y., L. Hu, et al. "Influence of silica particle internalization on adhesion and migration of human dermal fibroblasts." Biomaterials **31**(32): 8465-74.

Mina Wu

Birthdate: January 6, 1980

Birthplace: Hangzhou, China

EDUCATION:

Duke University (Durham, NC)

Ph.D., Biomedical Engineering, November 2011

University of Pennsylvania (Philadelphia, PA)

B.S.E Bioengineering, May 2002

HONORS & AWARDS:

BMES Travel Award, Biomedical Engineering Society, 2009

CBTE Fellowship, Duke University, 2004-2006

Tau Beta Pi, University of Pennsylvania, 2001-2002

Benjamin Franklin Scholar, University of Pennsylvania, 1998-2002

PUBLICATIONS:

1. M. Wu, F. Yuan, "Membrane Binding of Plasmid DNA and Endocytic Pathways are Involved in Electrotransfection of Mammalian Cells", *PLoS One*, **6**(6): e20923, 2011
2. M. Wu, F. Yuan, "Endocytic Pathways are Recruited for Electric Field-mediated DNA Uptake in a Cell-dependent Manner" (*in preparation*)
3. M. Wu, C. Chang, R. Dong, F. Yuan, "Investigation of Parallel Carbon Plate Electrodes for Improving Electric Field-Mediated Gene Delivery" (*in preparation*)

CONFERENCE PROCEEDINGS:

1. M. Wu, F. Yuan, "Membrane Binding of Plasmid DNA and Endocytic Pathways are Involved in Electrotransfection of Mammalian Cells", Biomedical Engineering Society Annual Meeting, Hartford, CT, Fall 2011 (Podium Presentation)
2. M. Wu, F. Yuan, "The Role of Endocytosis in the Uptake and Internalization of Plasmid DNA Following Electroporation", Biomedical Engineering Society Annual Meeting, Austin, TX, Fall 2010 (Poster Presentation)

3. M. Wu, F. Yuan, “Improving Electric Field-mediated Gene Delivery with Parallel Carbon Plate Electrodes”, Biomedical Engineering Society Annual Meeting, Pittsburgh, PA, Fall 2009 (Poster Presentation)
4. M. Wu, F. Yuan, “Effects of Pulsed Electric Field-Induced DNA Modifications on Transfection Efficiency of COS7 Cells”, Biomedical Engineering Society Annual Meeting, St. Louis, MO, Fall 2008 (Poster Presentation)